Mutation detection in TNFRSF13B encoding TACI in patients with Common Variable Immunodeficency

By

Edmund Poon

September 2006

MRes in Biomedicine

ProQuest LLC
789 East Eisenhower Parkway
P.O. Box 1346
Ann Arbor, MI 48106-1346

Abstract

Common Variable Immunodeficiency (CVID) is a primary immunodeficiency characterised by defects in immunoglobulin production and function. The molecular basis of CVID is not clear but a number of genes have recently been implicated. The TNF receptor superfamily member transmembrane activator and CAML interactor (TACI) is part of the APRIL-BAFF-BAFFR-BCMA-TACI system. It plays an essential role in the humoral immunity; especially in the maturation, proliferation and differentiation of B cells in human and mice. Recent reports suggest that mutations in TACI could form the molecular cause of a subset of patients with CVID. Multiplex capillary heteroduplex analysis, a mutation screening technique, was coupled with direct sequencing to analyse all five exons in TACI gene in a cohort of 26 CVID patients and in 47 healthy controls. The use of this screening strategy allowed high through-put analysis of samples with low cost but still achieved a high level of sensitivity. Through this approach, 2 individuals with CVID were identified with a heterozygous mutation that causes a functionally deleterious amino acid substitution, C104R, in TACI. To study the functional consequences of heterozygous C104R change, a lentiviral expression system was chosen to express mutant TACI in heterologous cell lines and B cell lines. TACI cDNA containing the C104R mutation was cloned into a lentiviral transfer vector. Lentiviral transduction of COS-7 cells

using vectors encoding either wild type or C104R mutant TACI showed expression of wild type but not of the C104R mutant. These studies suggest that mutations in the TACI gene may be pathogenic in CVID.

Acknowledgement

I am most grateful to my principal supervisors Dr. Bobby Gaspar and Dr. Chiara Bacchelli for their guidance, advice, enthusiasm and encouragement throughout the course of my project. It is both very exciting and rewarding to have them as my supervisors who have been truly committed to helping me in my learning process and made the experience nothing but enjoyable.

I would also like to express my special thanks to Sylvie Buckridge who I have been working close with and from whom I have learnt an immense amount. I am really thankful for her tireless enthusiasm, guidance and teaching me many new techniques.

Abbreviations

APRIL: A Proliferation Inducing Ligand

BAFF: B Cell Activation Factor of the Tumor Necrosis Factor Family

CAML: Calcium Modulator and Cyclophilin Ligand

CRD: Cysteine Rich Domain

CSR: Class Switch Recombination

CVID: Common Variable Immunodeficiency

eGFP: Enhanced Green Fluorescent Protein

FACS: Fluorescence Activated Cell Sorting

HA: Heteroduplex Analysis

Ig: Immunoglobulin

LNT: Lentiviral vector

MCHA: Multiplex Capillary Heteroduplex Analysis

NF-AT: Nuclear Factor of Activated T cells Transcription Factor

NF-κB: Nuclear Factor of Kappa B

PCR: Polymerase Chain Reaction

SNP: Single Nucleotide Polymorphism

TACI: Transmembrane Activator and CAML Interactor

TNF/R: Tumor Necrosis Factor / Receptor

TRAF: TNFR- Associated Factor

WT: Wildtype

1. Introduction

1.1. Common Variable Immunodeficiency Disease

Patients affected by Common Variable Immunodeficiency Disease (CVID) show a range of clinical manifestations and varied associated immunological defects. The common characteristics are: low serum immunoglobulin concentrations of IgG, IgA, IgE and frequently IgM; inability to produce antibody in response to vaccinations or antigen exposure; and recurrent bacterial infections resulting in frequent hospitalisation (Bryant et al. 1990;Cunningham-Rundles & Bodian 1999).

The age of onset in CVID is between 5 to 10 years old and 20-30 years old. However, recognition of the condition is often delayed due to the variety of illnesses resulting from an impaired immune system. Common recurrent infections in all patients include bronchitis, sinusitis and otitis. Many have a history of pneumonia and inflammatory gastrointestinal diseases; often infections lead to other complications with chronic lung diseases being most frequent (Cunningham-Rundles & Bodian 1999). Other phenotypes include granulomatous and lymphoproliferative diseases affecting about 10% CVID patients; and 20% have autoimmune diseases such as idiopathic thrombocytopenia purpura (ITP), autoimmune hemolytic anemia (AHA), systemic lupus erythematosus and vasculitis (Goldacker & Warnatz 2005). Susceptibility to malignancies and especially lymphoma are also increased in CVID patients. The clinical spectrum is extremely broad and it is therefore difficult to define CVID patients clinically.

The heterogeneity of the disorder is also observed at the immunological level and in the underlying mechanisms leading to immunodeficiency. Patients' B cells

vary in their ability to secrete immunoglobulin isotypes upon stimulation; with some patients unable to secrete both IgM and IgG; or only capable of producing IgM only or both (Bryant, Calver, Toubi, Webster, & Farrant 1990) suggesting defects within the class switch recombination (CSR) mechanism. However, better classification criteria to create homogeneous patient groups were needed and the ability of Ig secretion on its own does not truly reflect the diverse clinical aspect of CVID. Further immunologic studies revealed subgroups of patients which had defects in late B-cell differentiation stage by monitoring $CD27^+IgM^-IgD^-$ switched memory B cells in the peripheral blood lymphocyte pool. These findings showed a markedly low percentage of this cell type in this subgroup of CVID patients compared with healthy controls (Warnatz et al. 2002). Interestingly the number of $CD27^+IgD^+$ non-switched memory B cells varied in CVID right across the spectrum with patients having near to no memory B cells; to groups with defective switched memory B cells and normal numbers of non-switched memory B cells; and to increased numbers of $CD27^+IgD^+$ non-switched B cells (Piqueras et al. 2003). Somatic hypermutation of Ig genes in circulating peripheral B cells were also analysed. Analysis of the VH5 region of the Ig genes, has shown that even in some CVID patients with normal number of $CD27^+IgD^+$ memory B cells, little or no nucleotide changes were found (mutation frequency of 0.09) compared with controls with a mutation frequency of 1.8 (Agematsu et al. 2002); suggesting that in CVID memory B cells, the mechanisms of somatic hypermutation was non-functional. These diverse immunological defects make it harder to understand the fundamental cause of the disorder.

CVID is the second most prevalent primary immunodeficiency requiring medical attention, affecting 1 in 25,000 Europeans, with selective immunoglobulin-A

deficiency (sIgA-D) affecting approximately 1 in 600. Many families had been identified with closely related individuals affected by either CVID or sIgA-D. Analysis carried out on these families showed patterns of inheritance, suggesting a common genetic basis and pathogenic mechanism for these two deficiencies (Ashman et al. 1992). Patient case studies also showed the possibility of progression from sIgA-D to CVID (Espanol et al. 1996) further re-enforcing the idea that they may represent two phenotypic variants of the same disease spectrum. However, only 10% of CVID cases are familial showing autosomal dominant or recessive modes of inheritance and the majority are sporadic cases (Vorechovsky et al. 2000).

1.2. Genetic Defects in CVID Patients

1.2.1. Inducible Co-Stimulator (ICOS)

In recent years a number of genetic defects underlying CVID have been unraveled. One of the few molecular basis associated with causing CVID was described as the homozygous loss of the inducible co-stimulator (ICOS) gene. ICOS is expressed on activated T cells and resting T memory cells; it plays an important role in T cell costimulation providing additional stimuli when T cells become antigen activated (Hutloff et al. 1999). Functionally similar to CD28, it enhances a wide range of T cell responses: proliferation, up-regulation of molecules that mediate cell-cell interaction and synthesis of cytokines. In the context of CVID, the most important functions are enhancement of T cell help for B cell antibody secretion and effectively stimulating the release of interleukin (IL) - 10 – a B cell differentiation factor. (Hutloff, Dittrich, Beier, Eljaschewitsch, Kraft, Anagnostopoulos, & Kroczek 1999;Yoshinaga et al. 1999). T cells

expressing ICOS are found mainly in the apical light zone of germinal centers, where late differentiation of B cells into memory or early plasma cells occurs suggesting strong involvement (Beier et al. 2000). This led to two studies analyzing CVID patients of both sporadic cases and familial cases which show an autosomal recessive inheritance pattern. Collectively, 9 patients have been identified with a large homozygous deletion of ICOS and showing significant reduction in naïve, switched and memory B cells, characteristic of CVID. However, patients with ICOS deficiency only accounts for 2 % of all CVID cases to date (Grimbacher et al. 2003;Salzer et al. 2004).

1.2.2. CD19

CD19 is a co-stimulator forming a part of a membrane signal transduction complex with CD21. It plays an important role in the integration of innate immunity with adaptive immune recognition (Fearon & Carroll 2000). Foreign antigens recognized and bound to immunoglobulins on B cells are 'tagged' by complement fragments, C3d, which is covalently bound onto foreign antigens. The CD19/CD21 complex is then recruited to the antigen-Ig complex which then CD21 can bind the C3d. This elicits a co-stimulatory downstream signaling pathway via CD19 which regulates essential B cell functions: germinal center B cell differentiation; memory B cell development and maintenance; positive and negative selection of B cell subsets (Fearon & Carroll 2000).

The immunological abnormalities observed in CD19 deficient mouse model shows similar phenotypes compared to CVID. The mice show defective B cell activation by T cell dependent antigens, reduced number of switched memory B cells, and significantly decreased levels of serum immunoglobulin, a trademark characteristic

of CVID (Engel et al. 1995;Rickert, Rajewsky, & Roes 1995). However, the frequency at which CVID patients are associated with CD19 deficiency is approximately 1 %, only two homozygous null mutations of CD19 gene in 4 CVID patients from two families have been described (Salzer & Grimbacher 2005;van Zelm et al. 2006).

1.2.3. B cell Activation Factor of the Tumour Necrosis Factor (TNF) Family (BAFF)- Receptor

BAFF-receptor (BAFFR), a member of the TNF receptor superfamily, is expressed on resting B cells and T cells but is down-regulated in plasma cells. Its ligand, BAFF, is expressed as a type II transmembrane protein by macrophages, dendritic cells and neutrophils, which can then be subsequently proteolytically cleaved into a soluble form (Castigli & Geha 2006). The highly specific interaction of BAFF-BAFFR was investigated in BAFFR null mutant mice. The following immunophenotypes were observed: significant reduction of peripheral B cells; impaired T cell dependent responses; impaired germinal centre maintenance; impaired antibody class switching, normal IgA switching; and reduced numbers of marginal zone B cells (Schneider 2005). From analyzing the mice models, the important role implicated for BAFFR is supporting survival of transitional stage 2 (T2) B cells to mature B cell stages, as B cell distribution in bone marrow was normal (Thompson et al. 2001). Only recently has there been a case of homozygous deletion in the transmembrane region of BAFFR in one CVID family described (Salzer & Grimbacher 2005). Nonetheless, this just shows the diversity of genetic defects that underlies CVID.

1.3. Transmembrane Activator and Calcium-modulator and Cyclophilin Ligand (CAML) Interactor (TACI)

1.3.1. Structure and Signaling

TACI, encoded by the gene *TNFRSF13B*, is a member of the tumor necrosis factor receptor family (TNFR). A typical feature of a TNFR is the multiple copies of approximately 40-residue cysteine rich domains (CRD) in the extracellular domain which bind to the monomer-monomer interface of a trimeric ligand. The extracellular N-terminal domain of TACI possess two CRDs, each containing 6 highly conserved cysteines forming 3 intrachain disulfide bridges stabilizing the modules (Castigli & Geha 2006). The first CRD1 spans amino acid (aa) 32 to aa 67 and the second CRD2 is from aa 68 to aa 106. The two CRD domains in TACI each contain a feature called the DXL motif which consists of a conserved 6-residue sequence and they are required for the binding of two ligands: A proliferation-inducing ligand (APRIL), and BAFF (Day et al. 2005;Hymowitz et al. 2005).

An experimental study investigated whether TACI containing two CRD functions similar to a typical multi-domain TNFR. The contribution of CRD1 and CRD2 of TACI towards ligand binding was examined and it was found that the CRD2 on its own was sufficient for high affinity ligand binding to both APRIL and BAFF whilst still possesses functional signaling capabilities. This was demonstrated by a short isoform of TACI lacking CRD1 generated by alternative splicing (Hymowitz, Patel, Wallweber, Runyon, Yan, Yin, Shriver, Gordon, Pan, Skelton, Kelley, & Starovasnik 2005). The dual specificity of TACI for BAFF and APRIL was revealed in a co-crystal structure of APRIL.TACI analysis. A short β-hairpin structure formed with the DXL-motif was

required for BAFF ligand binding; but the presence of a hydrophobic core pocket enable the binding of APRIL too.

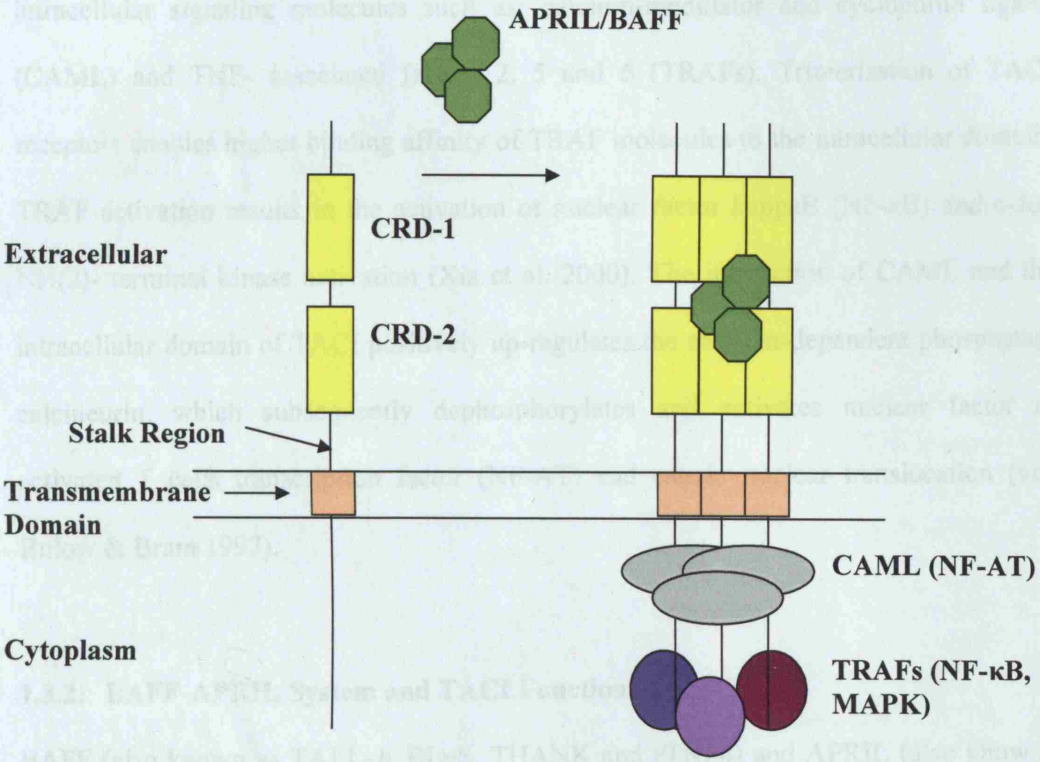

Figure 1.1. Schematic diagram of TACI structure and formation of trimeric ligand-receptor complex upon binding of APRIL/BAFF. Recruitment of intracellular signaling molecules, CAML and TRAFs, to the intracellular domain of trimeric TACI complex in a ligand-dependent manner initiates downstream signaling pathways: NF-AT, NF-κB and mitogen-activated protein kinase (MAPK) pathway.

Trimerisation of the TACI receptor forming a signaling complex upon binding to trimeric ligand of either APRIL or BAFF is shown in **Figure 1.1** (Bodmer, Schneider, & Tschopp 2002;Castigli & Geha 2006). This leads to the recruitment of intracellular signaling molecules such as: calcium-modulator and cyclophilin ligand (CAML) and TNF- associated factors 2, 5 and 6 (TRAFs). Trimerisation of TACI receptors enables higher binding affinity of TRAF molecules to the intracellular domain; TRAF activation results in the activation of nuclear factor kappaB (NF-κB) and c-Jun NH(2)- terminal kinase activation (Xia et al. 2000). The interaction of CAML and the intracellular domain of TACI positively up-regulates the calcium-dependent phosphatase calcineurin, which subsequently dephosphorylates and activates nuclear factor of activated T cells transcription factor (NF-AT) and causes nuclear translocation (von Bulow & Bram 1997).

1.3.2. BAFF-APRIL System and TACI Function

BAFF (also known as TALL-1, BLyS, THANK and zTNF4) and APRIL (also know as TRDL-1) both belong to the TNF ligand family member. As described before for BAFF, they both have typical features of type II transmembrane proteins, but unlike BAFF which is cleaved from the cell surface APRIL is processed intracellularly by furin convertase before secretion in soluble form (Lopez-Fraga et al. 2001). They are expressed by antigen-presenting cells (APCs), namely dentritic cells, monocytes and macrophages. TNF family ligands, such as BAFF and APRIL, are characterised by their C-terminal domain named TNF homology domain (THD) (Mackay et al. 2003).

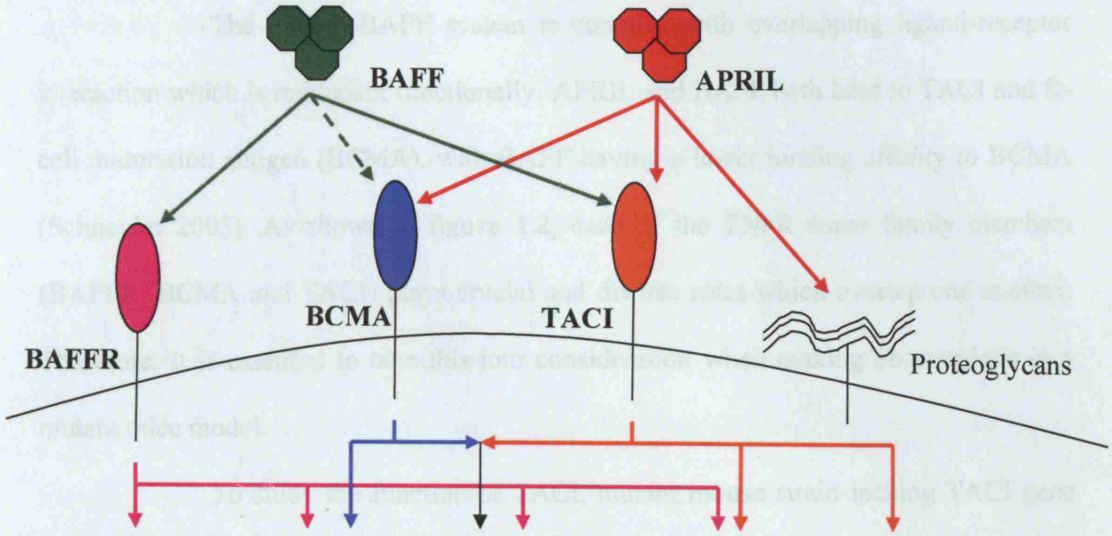

BAFFR only	BAFFR and BCMA	TACI and/or BCMA and BAFFR	BAFFR and TACI	TACI only
Peripheral B-cell survival	Plasma cell survival	Germinal centers	Ig switching (IgG, IgE)	Ig switching (IgA)
Marginal zone B cells		CD21 CD23 expression		Thymus-independent type II responses
T cell co-stimulation		Thymus-dependent responses		B-1 B cells (function, but not survival)
EFFECTS				

Figure 1.2. Adaptation from (Schneider 2005), illustrating ligand APRIL and BAFF interactions with their specific TNFR superfamily members. The table below describes the possible immunological function outcomes, assigned to each receptor, and their overlapping and redundant functions. However, the functional descriptions are not definitive as there are conflicting data existing.

The APRIL-BAFF system is complex with overlapping ligand-receptor interaction which is redundant functionally. APRIL and BAFF both bind to TACI and B-cell maturation antigen (BCMA), with BAFF having a lower binding affinity to BCMA (Schneider 2005). As shown in **figure 1.2**, each of the TNFR super family members (BAFFR, BCMA and TACI) plays crucial and diverse roles which overlap one another. Therefore, it is essential to take this into consideration when making observations in a mutant mice model.

To study the function of TACI, mutant mouse strain lacking TACI gene was generated by homologous recombination (Yan et al. 2001). Observations made in TACI null mice were enlarged spleen and lymph nodes with several fold increase in B cell numbers within these secondary lymphoid organs matching a lymphoproliferative disorder. The different compartments of the B cell population were also examined to determine the stage of B cell differentiation that TACI regulates. There were normal levels of pro-B cells, pre-B cells and immature B cells, all of which are found in the bone marrow, the primary lymphoid organ (Yan, Wang, Chan, Roose-Girma, Erickson, Baker, Tumas, Grewal, & Dixit 2001). In contrast, an increase in mature B cells in secondary lymphoid organs was observed. This suggests TACI acts as a negative regulator of B cell survival. Experimental data showing hyper-proliferation of B cells in TACI null mice upon stimulation with lipopolysaccharide (LPS), and inhibition of anti-CD40 antibody induced B cell proliferation by activation of TACI intracellular domain using agonistic mono-clonal antibodies to TACI (von Bulow, van Deursen, & Bram 2001) are evidence of TACI's role as a negative regulator, inducing apoptosis in these cells. As mentioned

before BAFFR, as shown in **Figure 1.2**, regulates peripheral B cell survival and activation, therefore hyper-proliferation of mature B cells can be explained by the positive regulation by BAFFR and also BCMA. Thus, TACI serves an important role in maintaining the homeostasis of B cell population.

Antibody production by B cells in TACI null mice was also examined. There are two types of responses: Thymus- dependent (TD) response and Thymus-independent (TI) response. TD responses result in B cell class switch recombination (CSR) in response to complex foreign protein; this process relies on T cell help through the co-stimulation of CD40 expressed on B cell surface and up-regulation of CD40-ligand expressed on T cells, following stimulation of T cell receptor (TCR) (Foy et al. 1996). CSR in thymus-independent responses occurs in the splenic marginal zone. This process involves the stimulation of B cells by APCs up-regulating IgG and IgA production and is thought to be mediated by BAFF and APRIL following antigen-stimulation of APCs (Litinskiy et al. 2002).

Immunisation of TACI null mice and normal mice revealed important role for TACI in T-independent type II humoral response. Significant abnormalities were observed when TACI null mice were immunized with TI type II antigen, there were markedly decrease in secretion of both IgM and IgG compared with normal mice (von Bulow, van Deursen, & Bram 2001). The lowered TI type II response did not improve upon higher dose of antigen administration. In contrast, the T-dependent response was not affected in TACI null mice. This suggests that TACI acts like a CD40 homolog, activating B cell CSR, by BAFF and APRIL stimulation, in the absence of T cell help within the marginal zones. Isotype IgA switching was also found to be abnormal when

naïve B cells from both normal and TACI$^{-/-}$ mice were compared in the same study (von Bulow, van Deursen, & Bram 2001).

TACI null mice model had many immunological abnormalities as well as phenotypic traits that are similar to defects observed in CVID. Besides lymphoproliferation signs such as splenomegaly, 15 % of TACI mutant mice developed lymphoma at the age of 7 to 8 months. Histological analysis also identified signs of autoimmune diseases with symptoms similar to systemic lupus erythematosus (SLE), an autoimmune disease mediated mainly by B cells (Seshasayee et al. 2003). These phenotypes observed in the mutant mice model are CVID associated diseases. The functional analysis of TACI deficient mice strongly suggests TACI deficiency is one of the genetic causes of CVID.

1.4. Subset of CVID Patients Carry TACI Defect

In recent years, cohorts of CVID patients of both sporadic cases and cases from multiplex families were screened through a candidate gene approach to identify mutations in the gene encoding TACI, *TNFRSF13B*. In one of the two studies, 19 CVID patients and 16 IgA-D patients were screened for mutations in *TNFRSF13B*; as a result 4 patients with CVID and 1 with IgA-D were identified with heterozygous missense mutations in *TNFRSF13B* (Castigli et al. 2005). No mutations were found in 50 healthy controls. In these individuals, three different missense mutations- a single nucleotide substitution resulting in an amino acid change, were found; with one individual having an insertion mutation in the other TACI allele. All the patients had normal sequences in regards to BAFF, APRIL and BAFFR ruling out other sources of defects within the BAFF-APRIL

system. Family members of the patients were also screened for mutations in the TACI gene and found strong evidence was found of TACI mutations co-segregating with the phenotype of both CVID and IgA-D. This suggests IgA-D and CVID may have a common underlying molecular defect (Ashman, Schaffer, Kemp, Yokoyama, Zhu, Cooper, & Volanakis 1992).

A larger cohort of CVID cases were screened by Salzer et al (Salzer et al. 2005). A total of 162 unrelated individuals with CVID and 100 healthy individuals were screened. 135 of those were sporadic cases and they found four different mutations in 10 cases. 27 index individuals from families with a history of multiple cases of humoral immuno-deficiency were also screened and three families were identified each with a different mutation in TACI. In contrast, none of the mutations were detected in control samples. Putting together the two cohorts of CVID and IgA-D cases analysed the frequency of TACI mutations is approximately 10 %.

The preliminary data shown from the two studies indicates a strong association of TACI defects with a subgroup of CVID and IgA-D population. However, in order to determine the true frequency and nature of TACI defects in CVID a larger cohort of CVID patients must be screened for mutations. In doing so, potential mutations maybe identified allowing better assignment of clinical and immunological phenotypes; functional analysis of specific TACI mutations; thus creating homogeneous subsets of TACI deficiency.

1.4.1. Clinical and Immunological Phenotypes of TACI deficient CVID Patients

The clinical phenotypes presented by TACI deficient CVID patients were heterogeneous; therefore CVID patients with mutations in TACI gene were not distinguishable from CVID with wildtype TACI gene based on phenotypic manifestations. CVID patients with mutant TACI all presented with typical characteristics such as recurrent infections of the respiratory and gastrointestinal tracts, including bronchitis, otits and sinusitis (Castigli, Wilson, Garibyan, Rachid, Bonilla, Schneider, & Geha 2005). Lymphoproliferative signs such as splenomegaly was most commonly observed in CVID individuals with TACI mutation Autoimmunity was reported at a higher frequency at 31% of individuals with CVID and mutations in TACI gene, compared with the whole population of CVID cases (Salzer, Chapel, Webster, Pan-Hammarstrom, Schmitt-Graeff, Schlesier, Peter, Rockstroh, Schneider, Schaffer, Hammarstrom, & Grimbacher 2005). However, autoimmunity with SLE symptoms observed in TACI null mutant mice was not observed in human with TACI deficiency and CVID.

Cellular phenotype was examined in TACI deficient individuals and observations of the B cell compartments were in contrast to TACI null mice. Mice model had an expanded peripheral B cell population (Yan, Wang, Chan, Roose-Girma, Erickson, Baker, Tumas, Grewal, & Dixit 2001), but in human with CVID and TACI defect peripheral B cell numbers were normal. In contrast to the TACI null mice, a subset of peripheral B cells, the switched memory B cells ($CD19^+CD27^+IgD^-$ B cells) were severly decreased (Salzer, Chapel, Webster, Pan-Hammarstrom, Schmitt-Graeff, Schlesier, Peter, Rockstroh, Schneider, Schaffer, Hammarstrom, & Grimbacher 2005). This suggests that the $TACI^{-/-}$ mutant mice model generated was not representative of the disease in human.

1.5. Mutation Screening Technique

Mutation detection by direct sequencing has always been the golden standard. However, direct sequencing is costly per sample, requires good quality and purified PCR fragments; and when large sample numbers and different fragments needed to be screened, can become labour intensive and time consuming. Mutation detection techniques can be catergorised into two groups 'specific' and 'scanning'. Specific techniques involve detection of mutational changes that have been characterised previously within a short length of DNA. Scanning techniques involve identifying sequence changes, within longer stretches of DNA, that haven't been previously characterised therefore able to detect both known and novel mutations.

The underlying genetic defects causing TACI deficiency have not been fully characterised. Screening of TACI exons in large cohorts of CVID patients and healthy controls is required to determine both the frequency and the nature of mutations. Therefore a fast, cost effective, specific and sensitive scanning method would be the most ideal, whilst retaining the ability to identify both known and novel mutations of various types (missense, nonsense and silent mutations; insertion and deletion alterations) in TACI gene.

The most common type of scanning technique is called conformation-based mutation scanning. This includes denaturing gradient gel electrophoresis (DGGE); denaturing high performance liquid chromatography (DHPLC) and single strand conformation polymorphism (SSCP). The advantages and disadvantages for using each of the methods vary. DHPLC is a highly sensitive method, capable of detecting single nucleotide substitutions in fragments from 150 to 700bp long, and has high-throughput

capabilities (Liu et al. 1998). DGGE and SSCP methods both also have high sensitivity; however they all have complicated initial optimisation processes. Factors such as temperature, pH, and primer design for amplification of DNA need to be optimized for each fragment of interest (Hayes et al. 1999;Highsmith, Jr. et al. 1999). The TACI gene consists of 5 different exons of varying length and GC contents; it would require extensive method optimisation for each of the exons.

Chemical cleavage of mismatches (CCM) and protein truncation test (PTT) are also common mutation screening method. PPT method requires RNA and is only useful in detecting premature translation termination (nonsense mutation) (Den Dunnen & Van Ommen 1999). The principle behind CCM is based on the ability of certain chemical reagents, such as potassium permanganate, to cut at the positions of mismatched bases but this technique requires handling of toxic chemicals and requires considerable expertise to obtain good results (Lambrinakos et al. 1999).

Heteroduplex analysis (HA) may be an ideal mutation screening method. HA is relatively inexpensive to use and is capable of detecting all kinds of alteration in sequences whilst achieving high-throughput, high sensitivity and low false positives/negatives (Hoskins et al. 2003). HA requires little optimisation for screening of different fragments making it suitable for screening TACI gene in a large cohort.

1.5.1. Heteroduplex Analysis (HA)

HA is a conformational-based mutation screening technique. The principles underlying HA is its ability to detect sequence differences between a 'reference' DNA fragment and a 'test' DNA fragment, suspected to contain mutations, by utilising the conformational

properties in heteroduplex species that are formed. Both homozygous and heterozygous mutations can be detected by HA. The method requires the amplification of 'reference' DNA fragments and 'test' DNA fragments from genomic DNA by PCR using fluorescently labeled primers. 'Reference' DNA will be wild-type TACI DNA fragment from healthy controls and 'test' DNA will be TACI DNA fragment from patients, that are being screened for mutations. PCR products of reference DNA and test DNA are then mixed together, denatured and allowed to reanneal slowly to allow the formation of homoduplexes and heteroduplexes (**Figure 1.3**)

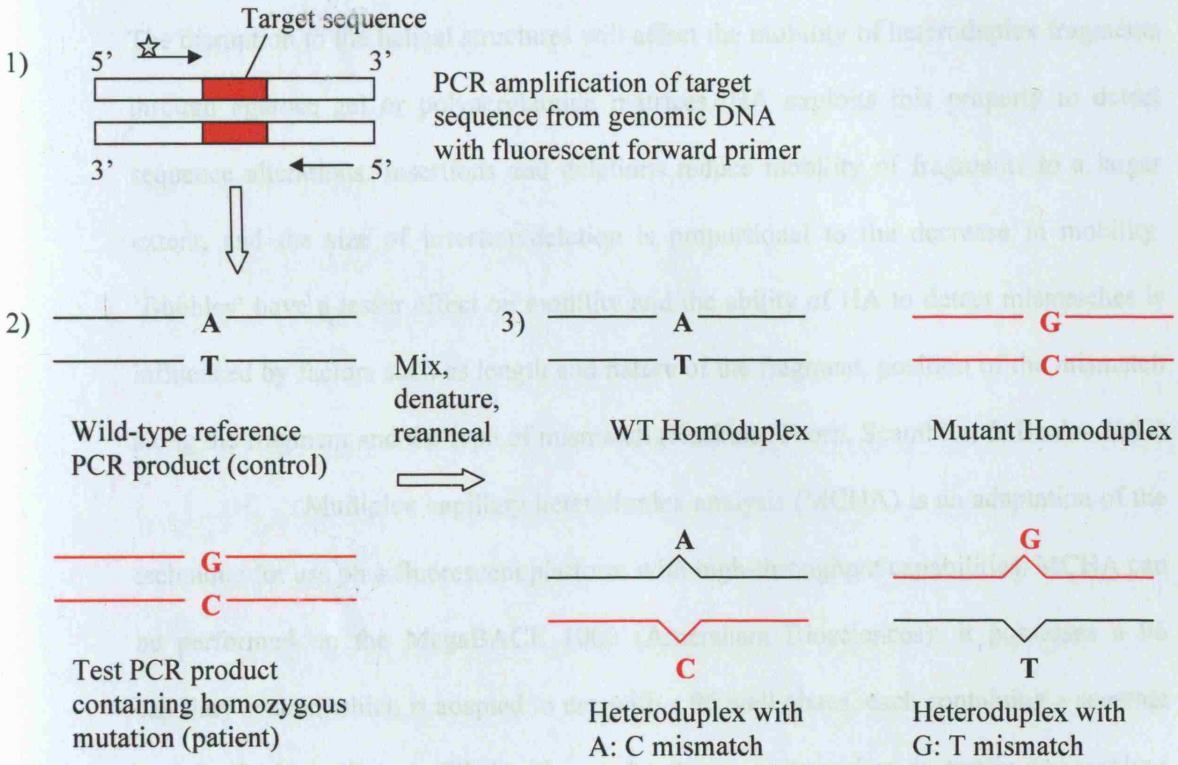

Figure 1.3. Heteroduplex and homoduplex formation. For illustration, PCR amplified test DNA contains a homozygous A to G substitution. When mixed with wild-type reference PCR product four species are formed: two homoduplexes and two heteroduplexes.

For test DNA that contains a heterozygous mutations, heteroduplexes and homoduplexes species shown in **Figure 1.3** are formed upon amplification by PCR. HA is able to distinguish heteroduplexes containing a small insertion or deletion in one of the strand of double stranded helices or containing mismatches, from homoduplexes, by the differences in conformation the helices adopt. There are two types of heteroduplex depending on the nature of the mutation present in the double helix. The presence of a small insertion or deletion will result in a 'bulge' formed in the heteroduplex and a 'bubble' is formed at the location of mismatched bases (Bhattacharyya & Lilley 1989). The disruption to the helical structures will affect the mobility of heteroduplex fragments through agarose gel or polyacrylamide matrices. HA exploits this property to detect sequence alterations. Insertions and deletions reduce mobility of fragments to a larger extent, and the size of insertion/deletion is proportional to the decrease in mobility. 'Bubbles' have a lesser effect on mobility and the ability of HA to detect mismatches is influenced by factors such as length and nature of the fragment, position of the mismatch along the fragment and the type of mismatch (Hoskins, Thorn, Scambler, & Beales 2003).

Multiplex capillary heteroduplex analysis (MCHA) is an adaptation of the technique for use on a fluorescent platform with high-throughput capabilities. MCHA can be performed on the MegaBACE 1000 (Amersham Biosciences); it possesses a 96 capillary system which is adapted to use with a 96 well plates, each containing a separate sample. Each capillary is filled with non-denaturing polyacrylamide matrix and resolves DNA fragments in the same way as a standard gel electrophoresis apparatus whilst achieving higher sensitivity and resolution.

1.6. Lentiviral Based Vectors for Experimental Gene Transfer

1.6.1. What is Lentiviral Vector?

Lentiviral vectors are developed from wild-type lentivirus, a more complex class of retrovirus, for *in vitro* and *in vivo* gene transfer. Retroviruses are a group of RNA viruses packaged within a capsid and a viral envelope. The life cycle of wild-type retroviruses involves infecting cells and replication through a DNA intermediate by the processes of reverse transcription of RNA to DNA followed by integration into the host genome. Transcription and translation of proviral DNA generates new viral genomic RNA and structural components required for producing new virions. Lentiviral vectors are modified to allow the expression of transgene and are only capable of undergoing one round of transduction (infection). Therefore, lentiviral vectors are replication incompetent unable to produce new viral particles to infect further cells.

The most common lentiviral vector is based on human immunodeficiency virus- 1 (HIV-1). The features that make up HIV-1 provirus (viral DNA form) will be discussed first followed by the modifications made in the design of lentiviral vector systems. Wild-type lentiviruses share common features with other types of retroviruses. They contain long terminal repeats at the 5' and 3' ends of the viral genome (5'LTR and 3'LTR), which are responsible for the integration process into the host genome and also regulate viral gene expression by acting as promoter. In between the LTRs, there are three structural genes *gag, pol* and *env*. Group specific antigen (*gag*) gene encodes viral core protein which is subsequently cleaved into separate viral core components; RNA dependent DNA polymerase (*pol*) gene encodes viral replication enzymes; and envelope (*env*) gene encodes viral glycoprotein that is incorporated into the viral membrane

subsequently. It also contains a packaging sequence (Ψ) at the 3' end of 5'LTR which distinguishes viral RNA from host RNA and allows packaging into viral particles.

Lentivirus, such as HIV-1, has additional components. These are regulatory genes; *tat* which regulates transcriptional activity from 5'LTR; and *rev* protein interacts with rev response element (RRE) which regulates efficient expression of *gag* and *pol* as well as the up-regulation of viral RNA transport out of the nucleus into the cytoplasm; and efficient splicing of viral RNA. There are also four accessory genes *vpr, vpu, vif* and *nef*; however, they are not required for viral production *in vitro* (Kim et al. 1998). **Figure 1.4** illustrates a schematic diagram of wild-type HIV-1 showing the viral genomic arrangement of all the components.

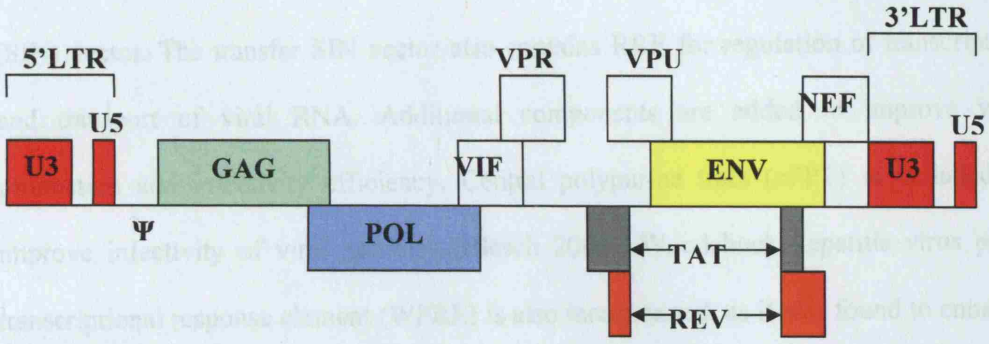

Figure 1.4. Diagram of a wild-type HIV-1. Lentiviral genome is flanked by two LTRs (each containing an U3 region and an U5 region) and consists of structural genes (*gag, pol* and *env*), regulatory genes (*tat* and *rev*), accessory genes (*vif, vpr, vpu* and *nef*) and packaging sequence (Ψ) located after 5'LTR.

A lentiviral gene transfer vector is a modification of wild-type HIV-1 to render it replication incompetent whilst retaining the essential functions to enable one infectious cycle for gene transfer *in vitro* or *in vivo*. The lentiviral vector system went

through a decade of development to maximize bio-safety whilst retaining effective gene transfer (Blesch 2004). The most advanced lentiviral vector system developed to date are called 'third generation'. The basis of lentiviral system is the separation of HIV-1 components into a transfer vector, a packaging construct and an envelope coding plasmid.

The transfer vector, used in this experiment as well, contains the following components: packaging sequence (Ψ) to provide packaging function of the viral RNA during viral production; primer binding site essential for reverse transcription to occur once in host cell; and modified LTRs for transcriptional regulation. The U3 region of 3'LTR has a deletion introduced; this prevents the possibility of replication competent production once inside host cells (Miyoshi et al. 1998), and results in a self-inactivating (SIN) vector. The transfer SIN vector also contains RRE for regulation of transcription and transport of viral RNA. Additional components are added to improve viral production and infectivity efficiency. Central polypurine tract (cPPT) is included to improve infectivity of viral particles (Blesch 2004). Woodchuck hepatitis virus post-transcriptional response element (WPRE) is also incorporated, as it was found to enhance transgene expression in target cells by mRNA stabilization (Donello, Loeb, & Hope 1998). The gene of interest is cloned within the vector's expression cassette; this consists of an internal promoter in this case the spleen focus forming virus (sffv), which regulates expression of transgene in target cells. **Figure 1.5a** illustrates the arrangements of the above components within a lentiviral transfer SIN vector.

The packaging construct is designed for providing packaging functions in *trans* to the transfer vector, but they lack the packaging signal therefore RNA transcribed from the construct is not encapsidated during viral production. The packaging construct

contains HIV-1 *gag* and *pol* genes providing essential viral core proteins and enzymes. It also contains *tat*, *rev* genes and RRE. 5'LTR is replaced by a heterologous promoter, cytomegalovirus (CMV) promoter and the 3'LTR with a polyadenylation site (pA). A separate plasmid also driven by CMV promoter and a pA at the 3' end contains the gene encoding for glycoprotein G vesicular stomatitis virus (VSV.G) envelope protein. The VSV.G gene replaces HIV-1 *env* gene, this is called pseudotyping the envelope of the hybrid virus particle produced (Manning et al. 1998). Pseudotyping broadens the range of cell infectivity and improves transduction efficiency. **Figure 1.5b** shows a schematic diagram of the packaging construct and the envelope coding plasmid.

Viral particle production is produced in packaging cell lines, such as 293T cells, through transient transfection of the transfer vector containing cloned transgene, packaging construct and the envelope encoding plasmid (Blesch 2004). Within the 293T cells transcription of viral RNA; translation of viral proteins and enzymes; and processing of viral components occurs. Viral components assemble together, maturation and budding results in the production of lentivirus particle. These lentivirus particles are then used for infecting target cells for gene transfer and as a result of the design features mentioned above are replication incompetent.

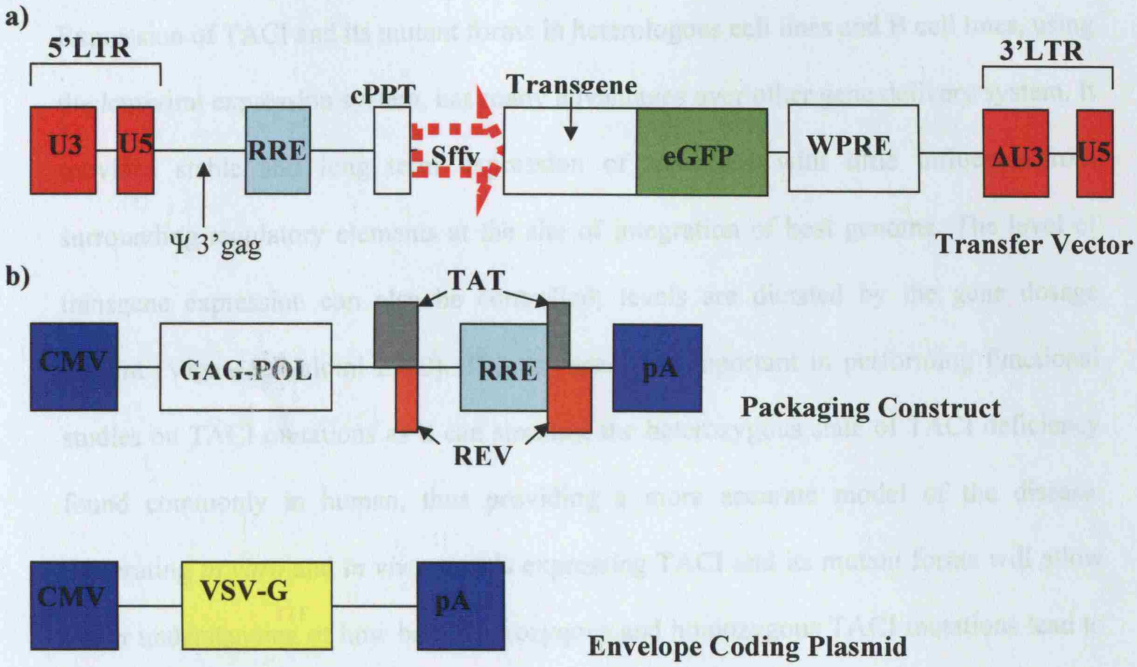

Figure 1.5. Schematic diagram of transfer lentiviral vector, packaging construct and envelope encoding plasmid. **a)** Transfer vector containing transgene and reporter gene (enhanced green fluorescent protein) driven by Sffv promoter. It also contains RRE, cPPT and WPRE components. Ψ sequence and a small 5' region of gag required for packaging. U3 region of 3'LTR has a deletion introduced (ΔU3) so that vector is self-inactivating. **b)** Both packaging construct and envelope coding plasmid is driven by cytomegalovirus (CMV) promoter and tagged with a polyadenylation sequence (pA) at 3' end. Packaging construct provides expression of viral core proteins and enzymes by *gag-pol* gene; *tat*, *rev* and RRE is present; but packaging signal is removed. Envelope coding plasmid expresses VSV G glycoprotein pseudotyping viral particle membrane.

1.6.2. Application of Lentiviral vector for generating *in vitro* models

Expression of TACI and its mutant forms in heterologous cell lines and B cell lines, using the lentiviral expression system, has many advantages over other gene delivery system. It provides stable and long term expression of transgene with little influence from surrounding regulatory elements at the site of integration of host genome. The level of transgene expression can also be controlled; levels are dictated by the gene dosage present (Vigna & Naldini 2000). This is especially important in performing functional studies on TACI mutations as it can simulate the heterozygous state of TACI deficiency found commonly in human, thus providing a more accurate model of the disease. Generating *in vitro* and *in vivo* models expressing TACI and its mutant forms will allow better understanding of how both heterozygous and homozygous TACI mutations lead to the disease phenotype.

1.7. Purpose of project

- Screening of CVID patient cohort to determine frequency and nature of TACI mutations

- Investigation of pathogenic features of specific mutations by generation of mutant TACI lentiviral constructs and expression in heterologous systems

2. Materials and Methods

2.1. Screening CVID patients for mutations in TACI using MCHA

2.1.1. Patients and Controls

The DNA from the cohort of patients was obtained from the Royal Free Hospital, London. Blood was collected from each of the patients and was sent to the Institute, where the DNA was extracted and made ready for this study. The cohort consists of 26 patients; 9 female and 17 male. Age ranges widely from 19 to 63 years old. Patients' immunoglobulin profiles and B cells numbers were measured at the time of diagnosis, as shown in **Table 2.1**. This information was originally used in the diagnosis of the type of immunodeficiency. 47 healthy control samples were obtained anonymously from National Blood Bank.

Patient Code	Sex	Age *(as at July 2006)*	Type of Immuno-deficiency	IgG Level at Diagnosis* (year taken from 1st blood test on PAS)	IgA Level at Diagnosis*	IgM Level at Diagnosis*	B cell Subsets CD19 % (date of test)
RH01	M	58	CVID	8.9 (10.01)	0.1	0.3	15 (29.11.05)
RH02	M	55	CVID	10 (10.01)	0.1	0.1	14 (03.11.05)
RH03	M	46	CVID	8.5 (11.02)	0.9	0.2	
RH04	M	63	CVID	9.3 (10.01)	0.3	0.2	1 (06.12.05)
RH05	M	43	CVID	6.7 (11.01)	< 0.1	< 0.1	28 (04.01.05)
RH06	F	40	CVID	9.6 (08.01)	< 0.1	0.2	14 (01.11.05)
RH07	F	29	CVID	4.7 (08.02)	0.3	0.3	4 (01.02.05)
RH08	F	46	CVID	9.3 (11.01)	<0.1	<0.1	12 (04.01.05)
RH09	M	DECEASED	CVID	10.0 (08.01)	<0.1	<0.1	
RH10	M	28	CVID	<0.1 (05.04)	<0.1	<0.1	26 (03.08.04)
RH11	F	19	CVID	8.2 (07.04)	0.1	0.1	3 (15.02.05)
RH12	M	DECEASED	CVID	5.7 (08.01)	0.2	2.9	
RH13	M	47	CVID	6.5 (08.01)	<0.1	0.1	
RH14	M	49	CVID	11.5 (01.03)	0.1	0.1	
RH15	M	54	CVID	0.2 (10.04)	<0.1	<0.1	51 (16.03.06)
RH16	F	35	CVID	4.4 (10.01)	0.8	1.4	16 (03.01.06)
RH17	M	63	CVID	10.0 (02.02)	<0.1	1.8	12 (08.02.05)
RH18	F	35	CVID	9.1 (02.02)	<0.1	3.1	7 (29.11.05)
RH19	M	30	CVID	7.1 (11.01)	<0.1	0.2	26 (30.05.06)
RH20	M	70	CVID	10.4 (07.01)	0.5	0.1	
RH21	F	61	IgG sub-class	8.7 (10.01)	1.3	0.8	0 (18.04.06)
RH22	M	25	CVID	8.7 (10.01)	0.1	0.1	2 (11.10.05)
RH23	M	52	CVID	7.6 (08.01)	<0.1	0.2	2 (14.06.05)
RH24	F	38	CVID	6.8 (08.01)	< 0.1	0.2	9 (08.03.05)
RH25	F	51	CVID	10.2 (10.01)	<0.1	<0.1	1 (07.12.04)
RH26	M	63	CVID	9.2 (07.01)	<0.1	<0.1	

Table 2.1. Patient details and measurements of their Immunoglobulin profiles and B cells numbers at the time of diagnosis of CVID

2.1.2. Polymerase Chain Reaction (PCR)

TACI exons were amplified by PCR. Approximately 100ng of template DNA was used in a 25µl reaction. Each PCR reaction mixture contains; 1x Mg free buffer, 2.5mM of $MgCl_2$; 2.5mM of each of the following dATP, dTTP, dCTP and dGTP; 1U of Taq DNA polymerase (all from Promega); exon 1 to 4 was screened separately, using the appropriate set of primers as shown in **Table 2.2**, 0.83µl of each of the forward and reverse primers (25pmol/µl) were used; finally the mixture was made up to a the final volume with 12.24µl of distilled water.

Table 2.2. Sequences of the forward and reverse primers used for amplifying TACI exons

TACI Exon	Forward Primer 5'- 3'	Reverse Primer 5'- 3'
1	AGTGCAGCCCAAGCACTAAT	AGTGTGTGGATCTGCTGTGG
2	CTGCTCCTCAGACAGAAAGGTT	CACACTGTACATCTCCTCCTGC
3	CTTTGATGTCCTTTGTGGTCAA	GCATTGTGGACTCTCCTGTTCT
4	ATGTGGATTGCTTGAGCCTAAT	TAGCAAGTAACAGGGATGAGCC

The forward primers were fluorescently labeled at the 5' end to enable detection when performing HA. Exon 1 and exon 2 primers are labeled with HEX; exon 3 and exon 4 primers are labeled with FAM.

PCR reaction mixtures were setup in 0.2ml PCR well plates (ABgene). Mastercycler® ep (eppendorf AG) was used to perform the reaction. For the DNA amplification of TACI exon 1, 2, and 4 the following thermal cycles were used: denature DNA template at 95°C for 2 minutes, followed by 35 cycles denature DNA at 95°C for 30

seconds, annealing of primers at 60°C for 30 seconds and at 72°C for 45 seconds for the elongation stage. After all the cycles the Mastercycler will hold the temperature at 4°C.

2.1.3. Touchdown Polymerase Chain Reaction

The PCR reaction mixture of TACI exon 3 was setup as the same as above stated but used an alternative technique. Touchdown PCR is another modification of conventional PCR that reduces amplification of non-specific sequences without having to carry out the process of time-consuming optimisation of primer annealing temperature (Don et al. 1991). The thermal cycles used for this technique was as follow: denature DNA at 95°C for 2 minutes, for the next 17 cycles denature DNA at 95°C for 30 seconds, annealing of primers at 68°C for 30 seconds decreasing 0.5°C every cycle and at 72°C for 45 seconds for elongation step; for another 25 cycles, 95°C for 30 seconds, 60°C for 30 seconds and 72°C for 45 seconds; followed by 10 cycles of, 95°C for 30 seconds, 59°C for 30 seconds decreasing 1°C after first 5 cycles and 72°C for 45 seconds; finally finishing off with 72°C for 2 minutes and holding temperature at 4°C when program finishes.

2.1.4. Gel Electrophoresis

TACI exon PCR products were routinely separated on a 2% agarose gel. Gel contains1g agarose (Invitrogen), 50ml of 1x Tris-Borate EDTA buffer and 5µl of 10mg/ml ethidium bromide. Hyperladder IV (Bioline) was used as a size standard. 2µl of loading buffer was added to 5µl of PCR product. Gels were run in 1x TBE buffer, at 100V for 40 minutes depending on the size of expected fragment. Fragments were visualized by the fluorescence of ethidium bromide under UV illuminator (UVtech) and photographed.

2.1.5. Forming Heteroduplexes

Mix 3µl of patient's PCR products with 3µl of wild-type control PCR products in a plate (ABgene). Then using the Mastercycler: heat mixtures at 95°C for 5 minutes and for the next 13 cycles 90°C for 2 minutes decreasing 5°C every cycle and finally holding at 25°C.

2.1.6. Preparation for Heteroduplex Analysis

Using a 96 well skirted plate (ABgene) add 7.5µl of sterile distilled water to each well. To detect mutation changes using HA in each patient the following components are required: patient's PCR product of amplified TACI exon alone ('unmixed sample'), its respective heteroduplexes ('mixed sample' formed in section 2.1.4), and the PCR product of the wild-type control used as the reference DNA in HA. Therefore preparation involves diluting 2.5µl of each of the above components in distilled water in the 96 well plate.

2.1.7. Performing Heteroduplex Analysis

HA is performed using the MegaBACE 1000 DNA Analysis System (Amersham Biosciences). Materials needed for each run on the machine are (all from Amersham): 6 tubes of non-denaturing long read matrix of at least 0.7ml centrifuged at 4000rpm for 4 minutes before use; 6 tubes of 1x linear polyacrylamide buffer (LPA buffer); a 96 well buffer plate containing 150µl of 1 x LPA buffer in each well, and the sample plate previously prepared.

For the Plate Setup the following electrophoresis parameters were used: sample injection voltage of 3KV; sample injection time of 30 seconds; run voltage of 7KV; and a

run time of 80 minutes. HA was then performed by following the protocols and programs displayed on the Instrument Control Manager software of the MegaBACE 1000.

2.1.8. Data Analysis

Data generated on the MegaBACE 1000 were analysed using MegaBACE Genetic Profiler software (Amersham). HA of the samples can be viewed as fluorescent signal traces called electropherograms. By analysing the peak morphology of unmixed, mixed and wild-type control, any deviation from the peak of control will indicate the presence of sequence alteration. The selected samples were then sequenced to identify and confirm the presence of mutation.

2.2. Sequencing to identify TACI mutations

2.2.1. PCR

The PCR mixture composition were the same as described in section 2.1.2, the primers used (25pmol/μl) are of the same sequences but are not fluorescently labeled. The thermal cycling programs used for the PCR reactions of exon 1 to exon 4 were the same as above.

TACI exon 5 was screened for mutations by direct sequencing only. TACI exon 5 was first amplified by PCR using the following forward and reverse primers (25pmol/μl): 5'ACCGTCACCCCTACCCTAGT and 5'CCTCCCTGACCCCCATTTAT. The rest of the PCR mixture was made up the same as previously described in 2.1.2. Touchdown PCR was used for amplifying exon 5, the following thermal cycles were used: denaturation at 94°C for 2 minutes; for next 25 cycles, denatution at 94°C for 30 seconds,

primer annealing at 72°C for 30 seconds decreasing 0.5°C every cycles and at 72°C for 45 seconds for elongation; for next 30 cycles, denaturing at 94°C for 30 seconds, followed by 60°C for 30 seconds, and at 72°C for 45 seconds; finally at 72°C for 2 minutes and hold temperature at 4°C. PCR products were then checked by gel electrophoresis, making sure there were no non-specific amplification and the band intensity was sufficed for subsequent sequencing.

2.2.2. Shrimp Alkaline Phosphatase (SAP)/ Exonuclease I treatment

PCR products were cleaned-up by breaking down single-stranded DNA and inactivation of free dNTPs by dephosphorylation. A 15µl total volume reaction was prepared per PCR product using 2 U of SAP (USB), 2 U of exonuclease I (*E.coli,* Epicentre), 5µl of PCR product and 7.9µl of dH_2O to make up the rest of the volume. The reaction was performed at 37°C for 60 minutes to activate enzymatic reactions followed by deactivation of enzymes at 80°C for 15 minutes.

2.2.3. Cycle Sequencing

For each sample to be sequenced two separate cycle sequencing reactions were made. Both reactions have a total volume of 10µl containing: 2µl of Big Dye ® Terminator v3.1 (from Cycle Sequencing Kit, Applied Biosystem), 1µl of 5x sequencing buffer (from the same kit), 3µl of cleaned PCR product, 3µl of dH_2O and 1µl of either the forward or reverse primers used in 2.2.1, but diluted 1 in 5 with dH_2O to a concentration of 5pmol/µl.

The mixtures were prepared in PCR plates (ABgene) and were centrifuged before using the following thermal cycling program to carry out cycle sequencing: temperature

was raised to 96°C for 10 minutes; for the next 31 cycles, denaturation of double-stranded DNA at 98°C for 45 seconds, primer annealing at 50°C for 10 seconds and 60°C for 4 minutes. The 'ramp speed' (the rate at which temperature is increased or decreased) was halved after the first of the 31 cycles. Finally temperature was held at 4°C.

2.2.4. Purifying of Sequencing Reactions by Gel Filtration

MultiScreen Filtration System (Millipore) was used to purify sequencing reactions. Filtration columns were made by adding Sephadex G-50 (Sigma) to the provided MultiScreen column loader. Using the scraper provided wells was filled in evenly and any excess resin was taken off. Then a 96 well MultiScreen HV Plate was aligned upside-down on top of the column loader. Resin was then released into the wells of the plate by inverting both the plate along with the column loader. 300µl of dH_2O was then added to each well to swell resin and was left at room temperature for 3 hours.

The HV plate was then placed on top of a 96 well skirted plate (ABgene) using a centrifuge alignment frame (Millipore) and was centrifuged at 2850 rpm for 5 minutes to pack the resin columns. Contaminants left in the resin was removed by pipetting 150µl of dH_2O to each well and centrifuged again at 2850 rpm for 5 minutes. Using a new 96 well skirted plate, sequencing reactions from 2.2.3 was added on to the centre of each sephadex column and was eluted by centrifuging at 2850 rpm for 5 minutes. Plates containing samples were sealed and ready for reading using the MegaBACE 1000.

2.2.5. Sequencing on MegaBACE 1000

The same MegaBACE 1000 DNA Analysis System (Amersham Biosciences) was used. Materials used were: a 96 well plate containing 150µl of 1xLPA (Amersham) in each well; 6 tubes with 2ml of 1xLPA in each; 6 tubes of MegaBACE Long Read Matrix (denaturing, Amersham) which was centrifuged at 4000 rpm for 4 minutes prior to use.

For the Plate Setup the following electrophoresis parameters were used: sample injection voltage of 3KV; sample injection time of 60 seconds; run voltage of 9KV; and a run time of 100 minutes. Sequencing was then performed by following the protocols and programs on the Instrument Control Manager software of the MegaBACE 1000.

2.2.6. Sequence Analysis

Sequencher 4.6 (Genes Code Corporation) software was used to analyse the data files generated from MegaBACE 1000. Reference amplicon sequences were imported into Sequencher and sample sequences were aligned against the corresponding TACI exon amplicon. Mutations were identified by the software automatically calling bases that are different, but usually the chromatograms of each sequence read were checked manually to distinguish ambiguities, disagreements with the reference sequence. The presence of a mutation is only confirmed when: either or both the forward and reverse chromatograms were perfect with no background noise; or both the forward and reverse chromatogram shows the presence of mutation even though background is higher than expected; or mutation is present in a repeat in either forward or reverse sequences.

2.3. Cloning TACI cDNA with C104R mutation into a Lentiviral Vector

2.3.1. Lentiviral-IRES-eGFP Vector Plasmid

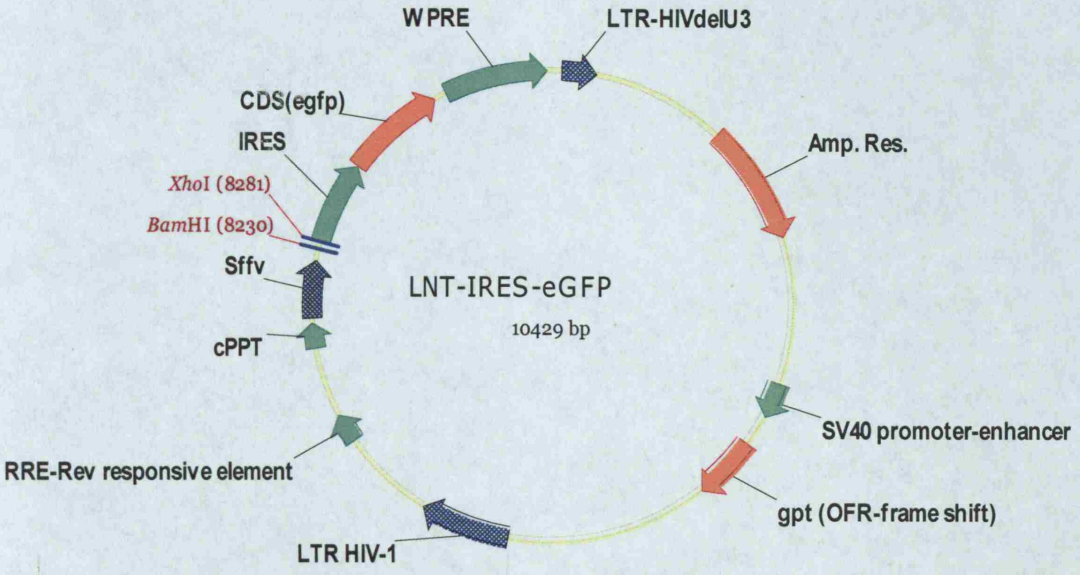

Fig 2.1. Circular map of lentiviral transfer vector (LNT-IRES-eGFP) containing HIV-1 derived long terminal repeats (LTR). U3 region of 3'LTR has a deletion introduced. It also contains rev response element (RRE), spleen focus forming virus (Sffv) internal promoter, Woodchuck hepatitis virus post-transcriptional regulatory element (WPRE), central polypurine tract (cPPT), enhanced green fluorescent protein (eGFP) reporter gene and an internal ribosome entry site (IRES). Restriction sites XhoI and BamHI are also shown.

LNT-IRES-eGFP is a HIV-1 based lentiviral transfer vector plasmid as shown in **Figure 2.1.** TACI insert containing the C104R mutation was cloned in between the Sffv promoter and the IRES component. The insert would ligate to the 3' blunt end created by cutting at the BamHI site followed by blunting reaction and the 5' overhang

created by XhoI digestion. The plasmid contains all the components of a third generation lentiviral transfer vector that can be used to produce viral particles in a packaging cell line.

2.3.2. pCR 3-TACI cDNA Vector

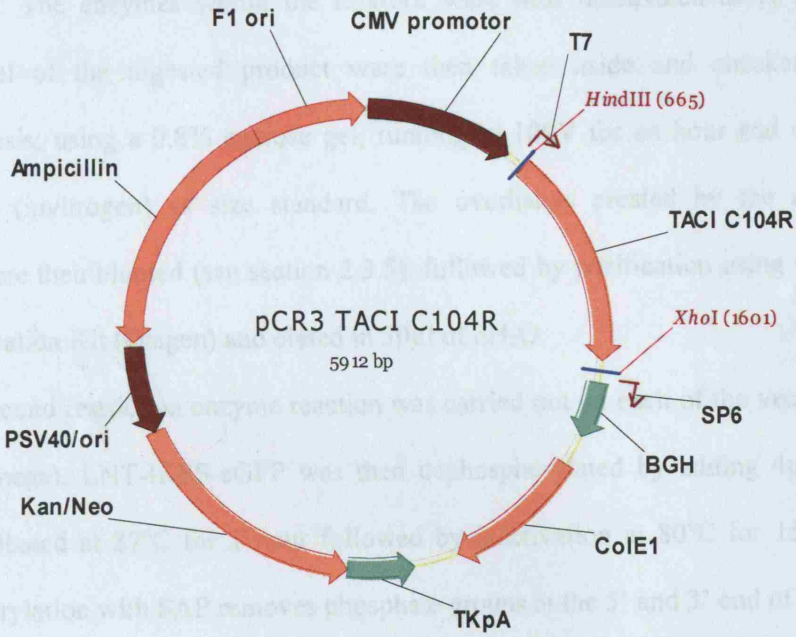

Fig 2.2. Circular map of pCR3 expression vector with full length TACI cDNA with C104R mutation cloned into the vector's multiple cloning sites. Restriction sites HindIII and XhoI are shown.

pCR3 TACI-C104R was a gift, ready for use in this study. The TACI insert containing the C104R mutation was the only interest of the plasmid and the aim was to cut the TACI insert out of the plasmid using the HindIII and XhoI restriction sites. The HindIII overhang was blunted. The resulting insert with 5' blunt end and 3' XhoI overhang was ligated to the digested transfer vector described in 2.3.1.

2.3.3. Cloning of TACI C104R cDNA into Lentiviral (LNT)-IRES-eGFP Vector

Restriction enzymes were used to cut the vectors at specific restriction sites- a highly specific recognition sequence which the enzyme will bind to the DNA and break the sugar-phosphate backbone of the double helix. LNT-IRES-eGFP vector and pCR 3-TACI cDNA vector were digested overnight with BamHI and HindIII (both from Promega), respectively. The enzymes within the mixture were heat inactivated at 70°C for 10 minutes. 5µl of the digested product were then taken aside and checked by gel electrophoresis; using a 0.8% agarose gel, running at 100V for an hour and using 1kb plus ladder (invitrogen) as size standard. The overhangs created by the restriction enzymes were then blunted (see section 2.3.5), followed by purification using QIAquick PCR Purification Kit (Qiagen) and eluted in 30µl of dH_2O.

A second restriction enzyme reaction was carried out on each of the vectors using XhoI (Promega). LNT-IRES-eGFP was then dephosphorylated by adding 4µl of SAP (USB) incubated at 37°C for 1 hour followed by inactivation at 80°C for 15 minutes. Dephosphorylation with SAP removes phosphate groups at the 5' and 3' end of the vector backbone to prevent self-ligation. Gel electrophoresis was then carried out on the two digests, using a 0.8% agarose gel running at 80V for 2 hours. The recipient lentiviral backbone and the TACI C104R cDNA insert were purified by excising the agarose gels containing the corresponding bands using a UV trans-illuminator (UVP) and a scalpel. The DNA was purified by gel extraction using QIAquick Gel Extraction Kit (Qiagen) and was ready for ligation of TACI C104R insert into the lentiviral-IRES-eGFP backbone.

2.3.4. Restriction Enzyme Reaction

A variety of restriction enzymes (from either Promega or Biolabs) were ultilised in preparation of the vector and confirmation of the final products. A typical reaction mixture was setup as follow: 0.1U/µl of restriction enzyme, 1x of the appropriate buffer, plasmid DNA and dH_2O was used to make up the rest of the volume. Mixture was incubated at 37°C for at least 6 hours, preferably overnight, for complete digestion. The enzymatic reaction was inactivated by heating at 70°C for 15 minutes when required.

2.3.5. Blunting

Overhangs created in the lentiviral vector and in pCR3-TACI C104R vector were blunted by adding 2U of Klenow enzyme (Roche) and 5µl of 100mM dNTPs mix (Promega) into the volume of digested vector. It was then incubated for 25 minutes at room temperature.

2.3.6. Purification Kit Protocol

QIAquick PCR Purification Kit (Qiagen) was used to purify the linear vectors from previous enzymatic reactions by following the manufacturer's instructions. The DNA were then eluted in 30µl of dH_2O.

2.3.7. Gel Extraction Kit Protocol

Agarose gel containing the band of interest was excised into clear 1.5ml eppendorf tubes. The weight of the gels was measured by subtracting the weight of the tubes from the total weight. Gels shouldn't be too large and any excess agarose not containing DNA should

be removed. DNA was then extracted by using QIAquick Gel Extraction Kit (Qiagen) following the manufacturer's instructions. DNA were finally eluted in 30µl of dH_2O.

2.3.8. Measuring Plasmid DNA Concentration

DNA concentrations were often measured and recorded using the ND-1000 spectrophotometer (NanoDrop Technologies). Before each measurement the ND-1000 was blanked with dH_2O and cleaned thoroughly before proceeding. Only 2µl of the eluted DNA were required to make a measurement.

2.3.9. Ligation

Two ligation reaction mixtures were setup: ligation of lentiviral vector with TACI C104R insert; and a control containing only lentiviral vector. For cloning of TACI C104R insert into lentiviral vector, the optimal molar ratio of vector to insert DNA was 1: 9.5. The size of insert is approximately 1.4kb and the size of vector is 10kb, the amount of vector used in the ligation was 50ng; using the following equation the amount of insert needed was calculated:

[(ng of vector x **kb size of insert)/ kb size of vector]** x **(molar ratio of insert/vector)**

= ng of insert

The first reaction mixture contained 50ng of lentiviral vector, 66.5ng of TACI insert, 1x ligation buffer (Roche), 1U of T4 DNA ligase (Roche) and making up the rest of the volume to a total of 15µl with dH_2O (Invitrogen). The second reaction mixture is a control and is exactly the same as the first mixture but omitting the TACI insert replacing it with dH_2O. Mixtures were vortexed and incubated at 16°C overnight.

2.3.10. Transformation

Two 14ml BD Falcon polypropylene round-bottom tubes were pre-chilled on ice, one for LNT-IRES-eGFP and TACI C104R ligation reaction and the other for LNT-IRES-eGFP only ligation control. Meanwhile a tube of XL1- Blue Supercompetent Cells (Stratagene) was thawed on ice. 40µl of cells were pipetted into each of the tubes and 0.7µl of β-mercaptoethanol (provided with cells) was added to each tube. The tube was then gently swirled every 2 minutes for the next 10 minutes. 2µl of each ligation reaction was added separately to the tube of cells. Tubes were then swirled again and incubated on ice for 30 minutes. The cells were heat-pulsed at 42°C in a water bath for 45 seconds exactly for the uptake of plasmids. They were immediately placed in ice for 2 minutes.

Supplements were added to 10ml of NZY Broth (1 L of ddH_2O containing 10g of NZ amine, 5g of yeast extract, 5g of NaCl, pH 7.5) before use: 200µl of 1 M $MgCl_2$, 100µl of 1 M $MgSO_4$ and 200µl of 20% glucose. The resulting supplemented NZY^+ Broth was pre-warmed to 42°C; 0.9ml of broth was added to each tube of transformed cells and incubated at 37°C for 1 hour shaking at 250 rpm.

Each of the culture was plated on a Luria-Bertani (LB) agar plate containing amplicillin (0.1mg/ml) by pipetting 50µl of culture onto the plate and was spread over the surface with a sterile plastic spreader. The remainder culture was concentrated by centrifuging at 2000 rpm for 5 minutes, removing 850µl of the supernatant and cells were resuspended. The rest of the cells were plated onto a second LB agar plate. They were then sealed and incubated overnight at 37°C.

2.3.10.1 Miniprep

The plated transformed cells formed colonies overnight. Individual colonies were then picked with a sterile loop; 5ml of LB broth (Sigma) containing 50mg/L of amplicillin was inoculated and incubated overnight (16 hours maximum) at 37°C shaken at 250 rpm. Cells were harvested by centrifugation at 4000rpm for 20 minutes, forming a cell pellet. Supernatant was discarded safely. QIAprep Spin Miniprep Kit (Qiagen) was used to purify plasmid DNA from the harvested cells following the manufacturer's instruction. Finally plasmid DNA were eluted in 30µl of distilled water.

2.3.10.2 Megaprep

Plasmid DNA were verified for the presence of cloned gene of interest. A larger quantity of the verified plasmid DNA was then prepared. First 5ml of LB broth (Sigma) containing 50mg/L of amplicillin was inoculated and incubated overnight (16 hours maximum) at 37°C shaken at 250 rpm. 1µl of the starter culture was then diluted in 200µl of fresh LB broth. The diluted culture was used to inoculate a volume of 500ml of LB medium with ampicillin in a 2 litre flask. Culture grew at 37°C for no more than 16 hours shaken at 250 rpm. Plasmid DNA were then purified using Qiagen Plasmid Mega Kit (Qiagen). Finally, plasmid DNA was collected by redissolving the DNA in 400µl of elution buffer (Qiagen) and the concentration measured. The process of dissolving precipitated DNA in elution buffer was repeated until DNA concentration measured decreases.

2.4. Expressing C104R mutant TACI in a heterologous cell line

2.4.1. African Green Monkey Kidney Cell Line (COS-7)

COS-7 was a gift, originally grown and maintained by Sylvie Buckridge. COS-7 is a fibroblast-like cell lines which grow and adhere to culture dish surfaces. COS-7 cells were cultured in 15cm culture dishes in 20ml of DMEM + GlutaMAX-1 medium (Invitrogen) containing 10% fetal bovine serum (heat inactivated; Sigma), 100μg/ml of penicillin and 100μg/ml of streptomycin antibiotics (Invitrogen) at 37°C. Above 90% confluency, the cell count in one 15cm culture dish was approximately 6 million.

COS-7 cell culture dish was split to maintain its growth. This involved warming DMEM medium and a 50ml aliquot of trypsin to 37°C. DMEM medium was removed from culture dish and rinsed with 10ml of 1x DPBS (Invitrogen). DPBS was then removed. 2ml of trypsin were added to each 15cm cell culture plates and incubated for 5 minutes maximum at 37°C. COS-7 cells were collected in 10ml of fresh DMEM medium in a falcon tube. It was centrifuged at 12000rpm for 5 minutes. Supernatant was removed and the cell pellet was resuspended in 30ml of fresh DMEM medium. Cell count was determined by a hemocytometer. 1/2, 1/5 or $1/10^{th}$ of total cells were then plated back on to culture dish in a total of 20ml of DMEM medium depending on the desired growth rate.

2.4.2. Electroporation

Plasmids were introduced into COS-7 cells by electroporation. Cells were confluent on the day of electroporation. The medium in the cell culture dishes was removed, cells were washed with DPBS and tryspinised as described in above section. After incubation at

37°C for 5 minutes with the trypsin cells were collected in DMEM medium and centrifuged at 12000rpm for 5 minutes. Cell pellet was then resuspended in 5ml per plate of special electroporation buffer (SEB; 120mM KCl, 10mM K_2PO_4/KH_2PO_4 pH 7.6, 2mM $MgCl_2$, 5mM Hepes pH 7.6 and 0.5% Ficoll 400; kindly prepared by Dr. Austen Worth). Cells were counted to make sure at least 13 million cells were available for each cuvette used for electroporation. Cells were centrifuged again at 12000rpm for 5 minutes. SEB was removed and 300µl per cuvette of fresh SEB was used to resuspend the cells. 20µg of each LNT-IRES-eGFP backbone vector, LNT-TACI C104R-IRES-eGFP vector and LNT-TACI WT-IRES-eGFP vector plasmids were added to separate 0.4 cm electrode cuvettes (Apollo). 300µl of cells suspended in SEB were added to each cuvette and incubated on ice for 4 minutes. Cells were electroporated using Biorad Genepulser at 250V and capacitance of 975µF. Cells were then incubated on ice for another 5 minutes and plated into a 15cm culture dish in 20ml of fresh medium per cuvette and left overnight at 37°C.

2.4.3. Detecting Enhanced Green Fluorescent Protein (eGFP) Expression

Olympus 1X70 fluorescent microscope was used to view fluorescence of expressed eGFP. The light bulb was switched on 20minutes prior to usage. Photographs of both green fluorescence and phase view were taken using the attached digital camera.

2.4.4. TACI Antibody Staining for Fluorescence Activated Cell Sorting (FACS)

Electroporated COS-7 cells were stained for FACS analysis to detect both wildtype and mutant C104R TACI expression. FACS analysis requires a minimum of $1x10^5$ cells per

staining. Therefore electroporated cells were washed and collected in 2ml of DPBS and counted. Cells were then centrifuged at 12000rpm, supernatant removed and resuspended in 400µl of DPBS. 200µl of cells were then transferred into each of the two FACS tube; one was the control and one was the 'test' cells stained for TACI. The test cells were incubated with 1.3mg of monoclonal rat IgG anti- human TACI (1A1 antibody; Abcam) at 4°C for 20 minutes in the dark. The test cells were then washed by adding 4.5ml of DBPS and centrifuged at 2000rpm for 5 minutes. Supernatant was decanted and cells were resuspended with 200µl of DPBS. 1µl of biotinylated rabbit anti-rat IgG secondary antibody (E0467; Dako) was added to both test and control cells. They were incubated at 4°C for 20 minutes in the dark. They were washed and resuspended in 200µl of DPBS as described above. 0.2mg of streptavidin-PE-Cy5 (BD Bioscience Pharmigen) was then added to the test and control cells and incubated at 4°C for 20 minutes in the dark. Cells were then washed and centrifuged as before removing supernatant by pouring it off. Cells were finally resuspended in 300µl of 1% paraformaldehyde, kept in the dark and ready for FACS analysis.

2.4.5. FACS analysis

FACS analysis was kindly performed by Joanna Sinclair using the FACS facilities in the Department of Hematology. Cells were gated upon granularity and size first. Then cells positive for eGFP expression were gated to analyse TACI staining within this population.

3. Results

3.1. Screening TACI gene in CVID patient cohort

	Changes found in screening CVID patient cohort					
	Exon 2	Exon 3		Exon 4	Exon 5	
	T27T	C104R	Intronic SNP	R202H	P251L	S277S
Nucleotide change at position	c.81	c.310	c.425+25	c.605	c.752	c.831
Type of nucleotide change	G to A	T to C	A to C	G to A	C to T	T to C
Synonymous (S) or Non-synonymous (NS)	S	NS	-	NS	NS	S
Amino Acid and position affected	Thr 27	Cys 104	-	Arg 202	Pro 251	Ser 277
Amino acid substituted by	-	Arg	-	His	Leu	-
Frequency of Homozygous change	10/24	0/26	1/26	0/26	3/25	9/25
Frequency of Heterozygous change	10/24	2/26	10/26	1/26		

Table 3.1. Summary of all the changes found in 26 CVID patient cohort. T27T change was found in exon 2; C104R and intronic SNP change found in exon 3; R202H change found in exon 4; and P251L and S277S found in exon 5. The nucleotide position and type of change are described and also their effects on amino acid sequence. The frequencies of homozygous and heterozygous change are shown. Frequency of P251L and S277S changes shown are total of both homozygotes and heterozygotes.

Mutation screening in 26 CVID patients from the Royal Free Hospital identified 6 different changes shown in **Table 3.1.** Changes T27T, intronic SNP, P251L and S277S are known polymorphisms and they are found at high frequencies as shown in the table. The nucleotide position of each change was first determined by analyzing sequencing results. The corresponding codons and its encoded amino acids were then determined. Depending on the nucleotide change, the mutation can either be non-synonymous or synonymous- nucleotide alteration resulting in an amino acid sequence change or resulting in no amino acid sequence change, respectively. (Individual results for each CVID patient are shown in Appendix A)

3.1.1. Heteroduplex analysis of *TNFRSF13B* in reference DNA controls

Exon 1, 2, 3 and 4 of TACI has its own designated reference DNA control used in HA. Using MCHA, each control DNA was analysed and shown in **Figure 3.1.** The electropherograms of all four exons are similar, each showing a single distinct, smooth sided peak. The reference DNA controls used consist of one homoduplex species, the wild-type TACI exon. Therefore, when resolved on the MegaBACE 1000 they travel through the matrix at the same speed and are detected at the same time. The peak observed in the electropherogram corresponds to their respective homoduplex DNA controls. The values shown on the x-axis of the electrophoregram is of no significance in this application but it shows the relative time point at which the fluorescently labeled DNA fragments were detected within the 'run' period. It is worth noticing that the time-point of detection of the same homoduplex in different 'runs' will vary. The y-axis represents the intensity of the fluorescent signal detected. In Figure 3.1a and 3.1b artifact

signals were seen, however, artifacts were easily distinguishable from the peak of interest. This is usually due to fragmented DNA debris or dye 'blobs' as a result of insufficient clean-up.

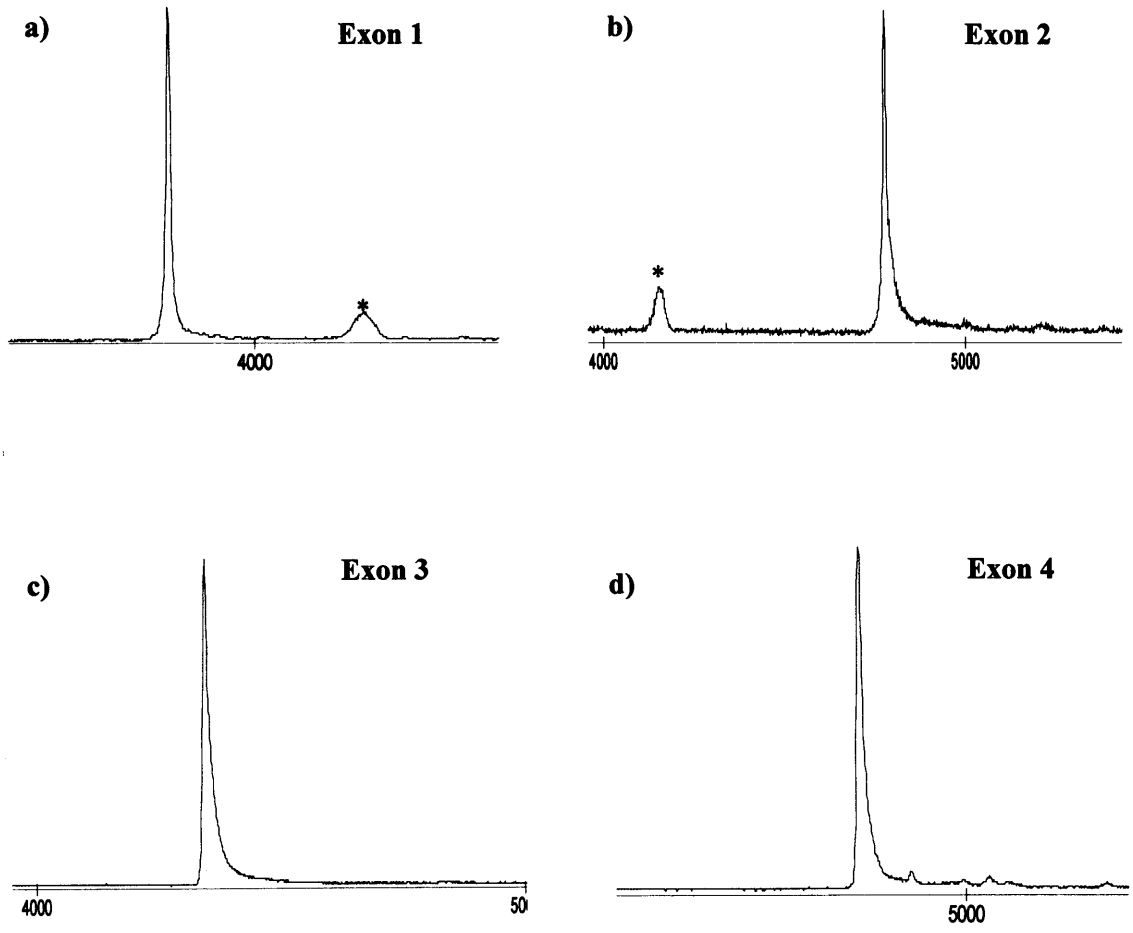

Figure 3.1. Typical heteroduplex analysis electrophoregram of the following reference DNA controls **a)** Wild-type TACI Exon 1 **b)** Wild-type TACI Exon 2 containing a known homozygous polymorphism (c.81G>A) **c)** Wild-type TACI Exon 3 **d)** and Wild-type TACI Exon 4. Asterisks (*) indicate artifacts considered as background noise signal.

3.1.2. Polymorphisms present in TACI gene

3.1.2.1 Heterozygous R202H a rare polymorphism found in TACI exon 4

Mutation screening of a 26 CVID patient cohort by HA; followed by subsequent sequencing of potential samples containing sequence alteration of TACI exon 4 revealed a rare heterozygous polymorphism (R202H) in patient RH13. **Figure 3.2**, shows the HA of patient's TACI exon 4 fragment. A subtle peak 'split' morphology was observed, a deviation from the peak morphology of the HA of reference DNA control. This shows the 'unmixed' sample containing two species of homoduplexes and two species of heteroduplexes; this results from the presence of a single heterozygous nucleotide substitution and the process of PCR. Due to a significant increase in the amount of wild-type homoduplexes present in the 'mixed' sample, a similar morphology was not observed as expected. DNA fragment of Patient RH13 was then sequenced to identify and confirm presence of mutation. **Figure 3.2d** shows the sequencing data in Sequencher analysis software. The base difference between reference DNA sequence and sequence data of RH13 was 'marked' by the software, identifying the polymorphism at the nucleotide 160 position within exon 4. It is a G to A substitution; and its position within TACI gene corresponds to nucleotide 605 (c.605G>A). This causes an amino acid sequence change at amino acid 202, substituting an arginine with histidine (R202H).

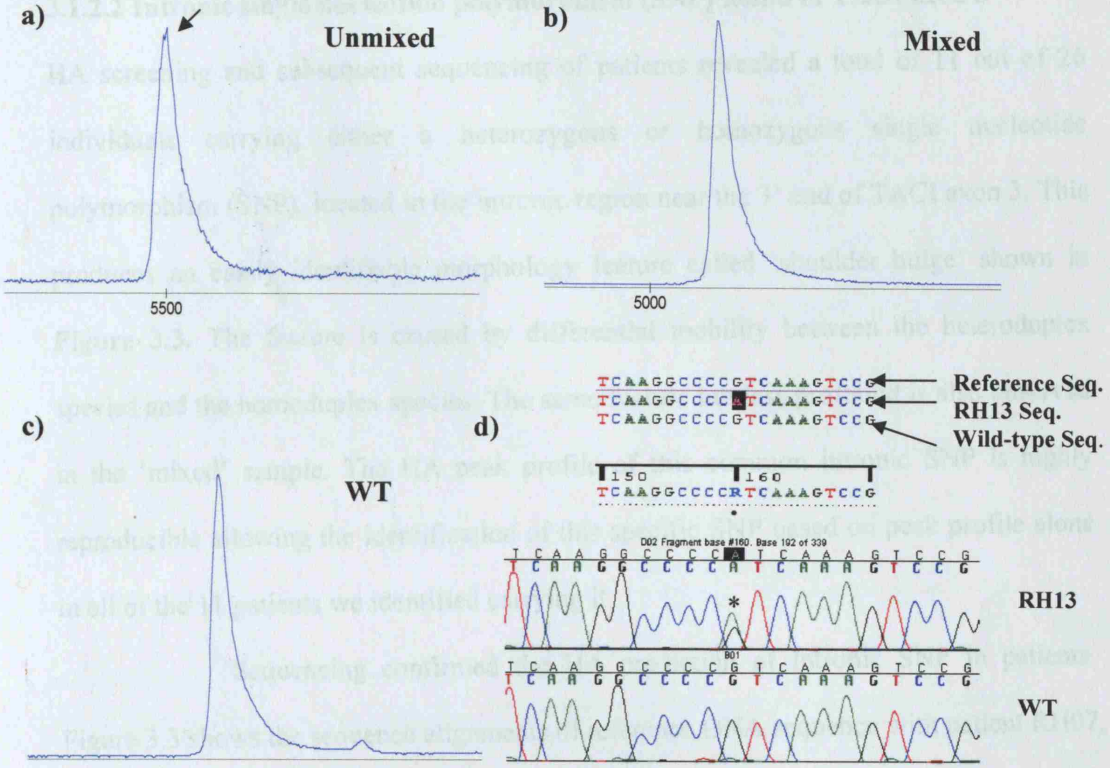

Figure 3.2. HA electropherograms and sequencing of TACI exon 4 of patient RH13 **a)** heteroduplex analysis of 'unmixed' TACI exon 4 fragments from patient RH13 showing a split peak morphology as indicated by arrow **b)** HA of 'mixed' DNA fragments from patient RH13 and from TACI exon 4 reference DNA control **c)** HA of TACI exon 4 reference DNA control only **d)** Top half shows sequence alignment of reference sequence with the sequencing of patient RH13 and wild-type control. The bottom half shows the electropherograms of the sequencing performed on RH13 and wild-type control. Asterisk (*) indicate location of nucleotide substitution of G to A.

3.1.2.2 Intronic single nucleotide polymorphism (SNP) found in TACI exon 3

HA screening and subsequent sequencing of patients revealed a total of 11 out of 26 individuals carrying either a heterozygous or homozygous single nucleotide polymorphism (SNP), located in the intronic region near the 3' end of TACI exon 3. This produces an easily identifiable morphology feature called 'shoulder bulge' shown in **Figure 3.3.** The feature is caused by differential mobility between the heteroduplex species and the homoduplex species. The same feature but less profound is also observed in the 'mixed' sample. The HA peak profile of this common intronic SNP is highly reproducible allowing the identification of this specific SNP based on peak profile alone in all of the 11 patients we identified carrying it.

Sequencing confirmed the HA prediction of intronic SNP in patients. Figure 3.3 shows the sequence alignments of reference DNA sequence with patient RH07, predicted to carry heterozygous intronic SNP. The polymorphism was found at nucleotide position 470 of TACI gene, 25 bases downstream the 3' end of exon 3. It is a nucleotide substitution of A with C, this intronic SNP is abbreviated as c.445+25A>C.

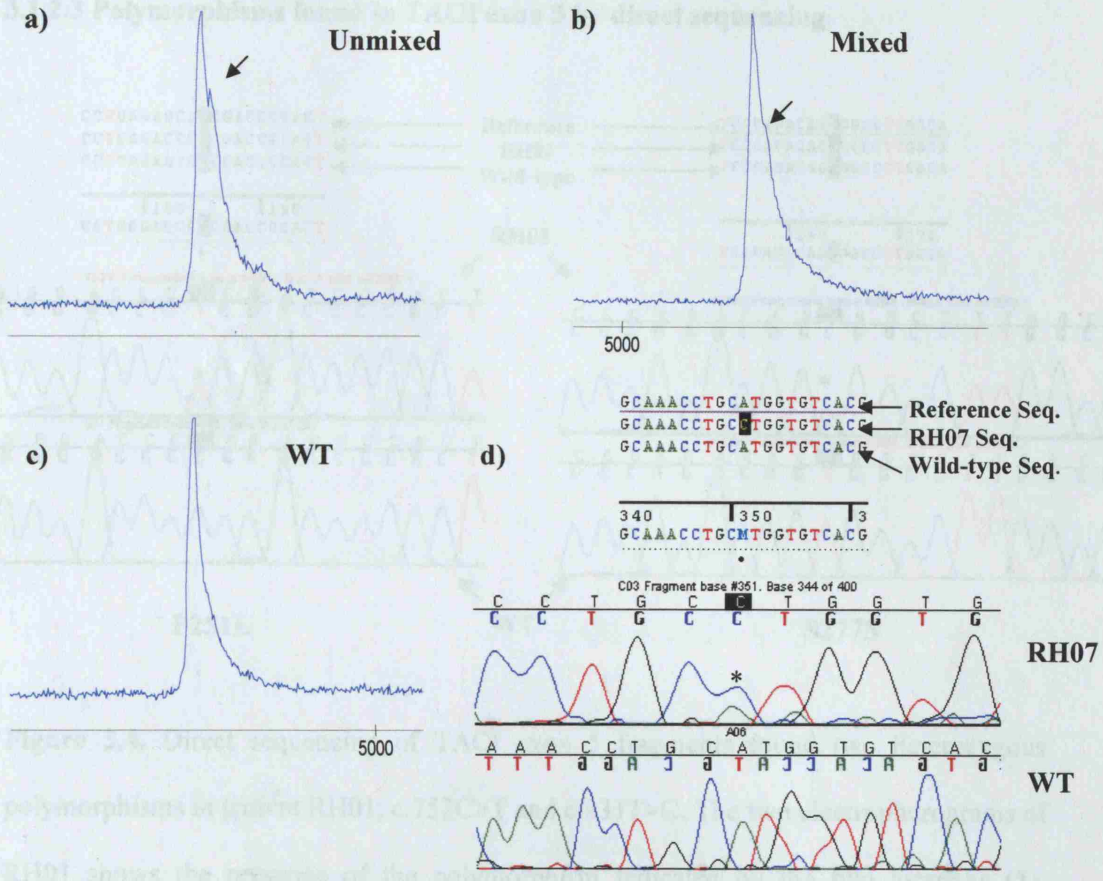

Figure 3.3. HA electropherograms and sequencing of TACI exon 3 of patient RH07 **a)** heteroduplex analysis of 'unmixed' TACI exon 3 fragments from patient RH07 showing 'shoulder bulge' morphology as indicated by arrow **b)** HA of 'mixed' DNA fragments from patient RH07 and from TACI exon 3 reference DNA control, arrow indicating morphology difference **c)** HA of TACI exon 3 reference DNA control only **d)** sequence alignment of reference sequence with the sequencing of patient RH07 and wild-type control. The electropherograms of the sequencing performed on RH07 and wild-type control. Asterisk (*) indicate location of nucleotide substitution of A to C.

3.1.2.3 Polymorphisms found in TACI exon 5 by direct sequencing

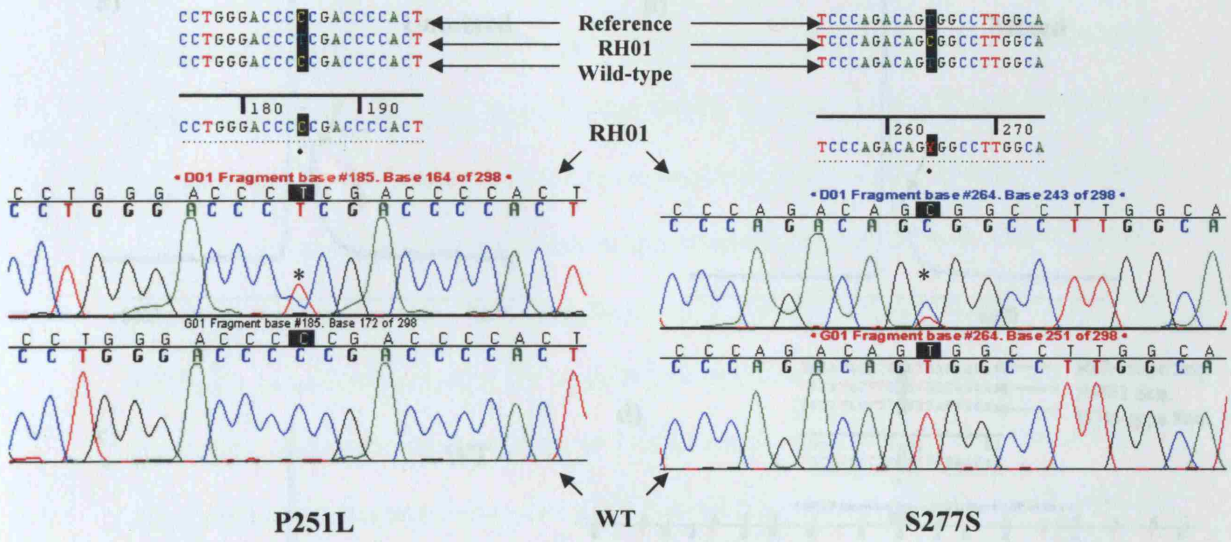

Figure 3.4. Direct sequencing of TACI exon 5 fragments found two heterozygous polymorphisms in patient RH01, c.752C>T and c.831T>C. The two electropherograms of RH01 shows the presence of the polymorphism indicated by the two asterisks (*). Sequence alignment with TACI exon 5 reference DNA control is also shown above the electropherograms.

P251L change resulted from a nucleotide substitution of C with T at position 752 of TACI gene shown in **Figure 3.4**; it was found in 3 out of 25 CVID patients sequenced. S277S resulted from a nucleotide substitution of T with C at position 831 of TACI gene; it was found at a greater frequency of 9 out of 25. S277S change is a synonymous sequence alteration; therefore serine 277 to which it corresponds is not affected. In contrast P251 change causes an amino acid substitution; proline 251 is replaced with leucine (P251L).

3.1.3. Screening of 26 CVID patients identified mutations in TACI gene

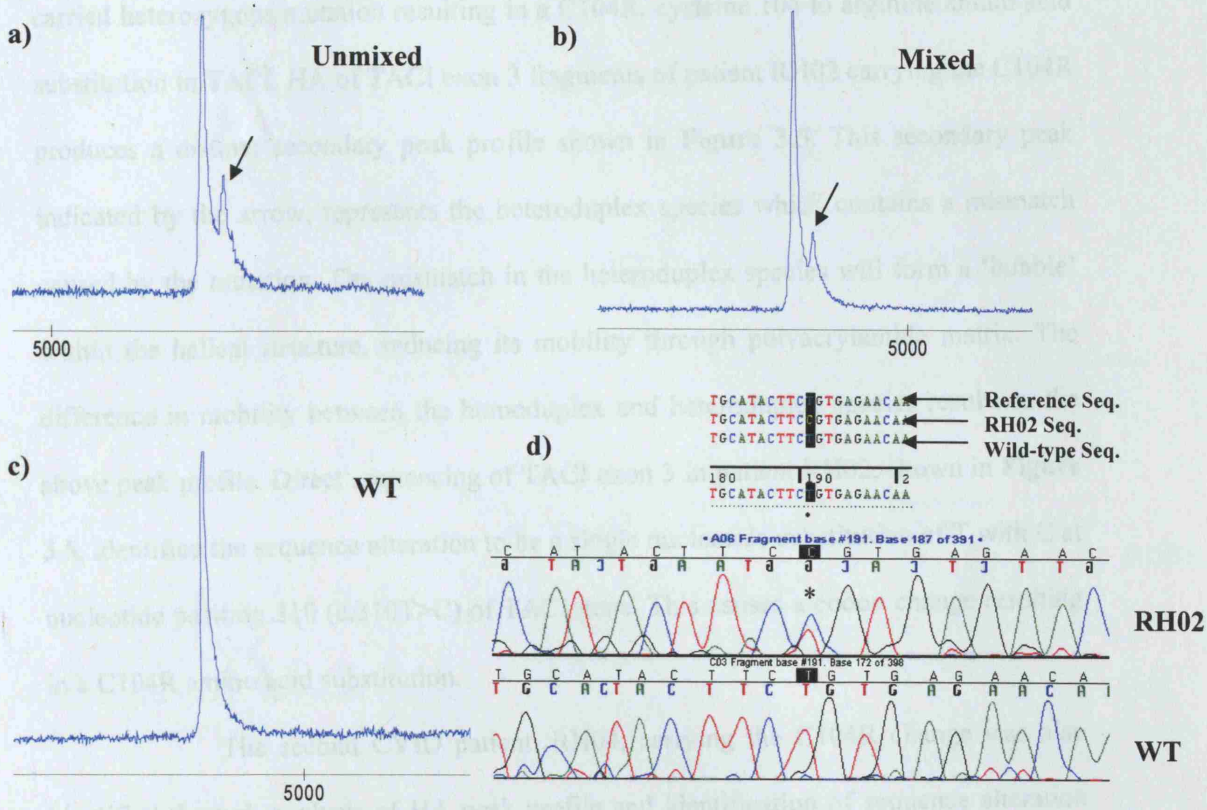

Figure 3.5. HA electropherograms and sequencing of TACI exon 3 of patient RH02 **a)** heteroduplex analysis of 'unmixed' TACI exon 3 fragments from patient RH02 showing secondary peak as indicated by arrow **b)** HA of 'mixed' DNA fragments from patient RH02 and from TACI exon 3 reference DNA control, arrow indicates secondary peak **c)** HA of TACI exon 3 reference DNA control only **d)** sequence alignment of reference sequence with the sequencing of patient RH02 and wild-type control. The electropherograms of the sequencing performed on RH02 and wild-type control are shown in the bottom half. Asterisk (*) indicate location of nucleotide substitution of T to C.

Heteroduplex analysis and subsequent sequencing confirmed 2 CVID patients out of 26 carried heterozygous mutation resulting in a C104R, cysteine 104 to arginine amino acid substitution in TACI. HA of TACI exon 3 fragments of patient RH02 carrying the C104R produces a distinct secondary peak profile shown in **Figure 3.5**. This secondary peak indicated by the arrow, represents the heteroduplex species which contains a mismatch caused by the mutation. The mismatch in the heteroduplex species will form a 'bubble' within the helical structure, reducing its mobility through polyacrylamide matrix. The difference in mobility between the homoduplex and heteroduplex species results in the above peak profile. Direct sequencing of TACI exon 3 in patient RH02, shown in **Figure 3.5**, identified the sequence alteration to be a single nucleotide substitution of T with C at nucleotide position 310 (c.310T>C) of TACI gene. This causes a codon change resulting in a C104R amino acid substitution.

The second CVID patient, RH04, carrying the C104R change was also identified through analysis of HA peak profile and identification of sequence alteration by direct sequencing. The HA of TACI exon 3 of patient RH04, in **Figure 3.6**, shows a similar peak profile to that of patient RH02 but with discrepancies due to the presence of another sequence alteration. The HA of 'unmixed' fragments resulted in a low intensity signal detected, this made analysis of the HA more difficult as morphology features are often distorted or concealed within background signals. A secondary peak was observed in both 'mixed' and 'unmixed' samples and a 'shoulder bulge' was also observed. Subsequent sequencing identified the presence of a heterozygous c.310T>C mutation (C104R) and heterozygous intronic SNP.

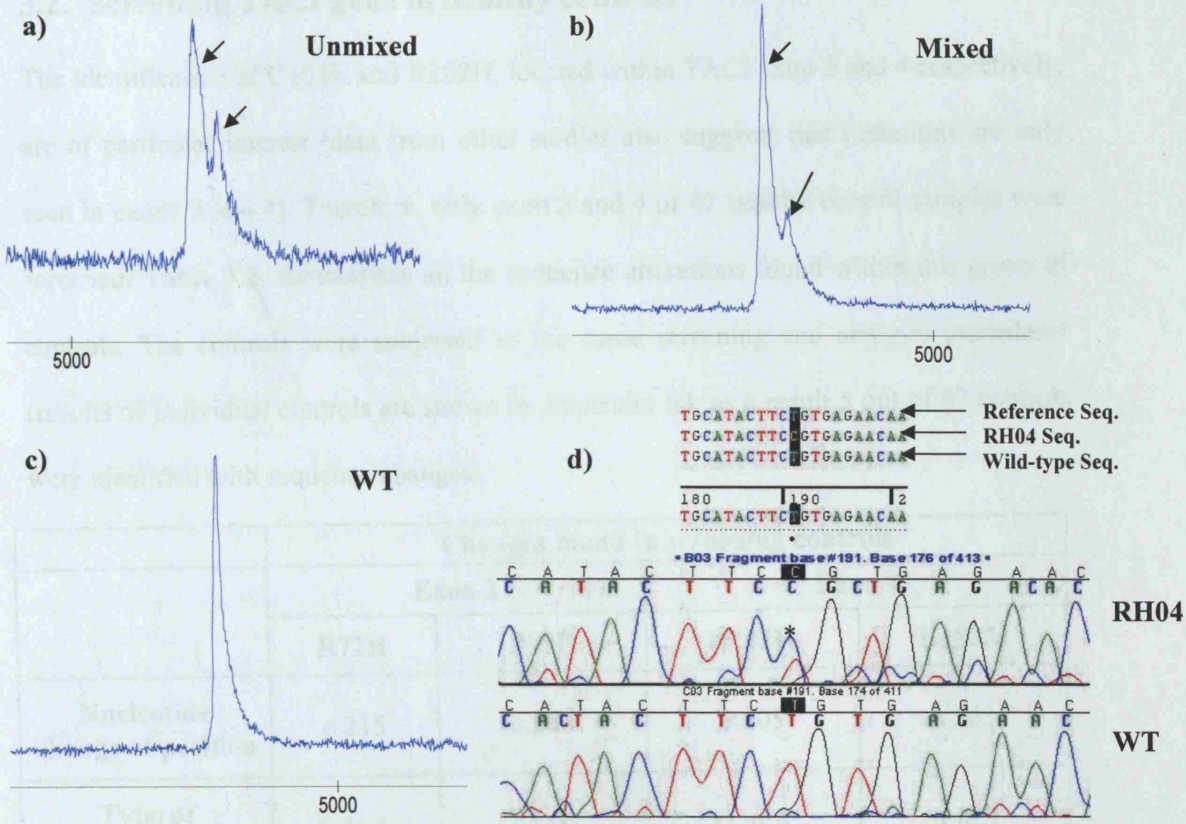

Figure 3.6. HA electorpherograms and sequencing of TACI exon 3 of patient RH04 **a)** HA of 'unmixed' TACI exon 3 fragments from patient RH04, arrows indicate locations of morphology features suggesting the presence of heterozygous mutations or polymorphisms **b)** HA of 'mixed' DNA fragments from patient RH04 and from TACI exon 3 reference DNA control, the same features were observed show by the arrows **c)** HA of TACI exon 3 reference DNA control only **d)** sequence alignment of reference sequence with the sequencing of patient RH04 and wild-type control. The electropherograms of the sequencing performed on RH04 and wild-type control are shown in the bottom half. Asterisk (*) indicate location of nucleotide substitution of T to C.

3.2. Screening TACI gene in healthy controls

The identification of C104R and R202H, located within TACI exon 3 and 4 respectively, are of particular interest (data from other studies also suggests that mutations are only seen in exons 3 and 4). Therefore, only exon 3 and 4 of 47 healthy control samples were screened. **Table 3.2,** summarises all the sequence alterations found within this group of controls. The controls were subjected to the same screening and analysis procedures (results of individual controls are shown in Appendix B); as a result 5 out of 47 controls were identified with sequence changes.

	Changes found in screening controls			
	Exon 3		**Exon 4**	
	R72H	**P97P**	**R202H**	**K188M**
Nucleotide change at position	c.215	c.291	c.605	c.563
Type of nucleotide change	G to A	T to G	G to A	A to T
Synonymous (S) or Non-synonymous (NS)	NS	S	NS	NS
Amino Acid and position affected	Arg 72	Pro 97	Arg 202	Lys 188
Amino acid substituted by	His	-	His	Met
Frequency of Homozygous change	0/47	0/47	0/47	0/47
Frequency of Heterozygous change	1/47	2/47	1/47	1/47

Table 3.2. Changes found in TACI gene exon 3 and 4 when screening 47 healthy controls. Four different changes were found (R72H, P97P, R202H and K188M). The table summarises the locations of nucleotide sequence changes and the effects it has. The frequency of the changes found is also shown.

Screening of TACI exon 3 in the controls identified two new changes R72H and P97P. Two healthy controls carried the heterozygous P97P change; this is a silent mutation because the nucleotide change has no affect on the codon that codes for proline. One individual carried a R72H change, position 72 is the first amino acid which TACI exon 3 encodes for; and arginine is found within the CRD1. Screening of TACI exon 4 also identified two changes R202H and K188M. One individual carried a heterozygous R202H change. Another control carried a new heterozygous K188M change not found in the cohort of CVID patient but at such low frequency in control samples analysed here it cannot be defined as a polymorphism without further evidence. Lysine 188 is located right after the transmembrane domain in the intracellular domain. The above table did not include the 34 intronic SNPs, homozygotes and heterozygotes, found in the healthy controls cohort.

3.3. Cloning of TACI gene containing C104R mutation into a lentiviral transfer vector

3.3.1. Restriction Enzyme Digestions of LNT-IRES-eGFP Vector

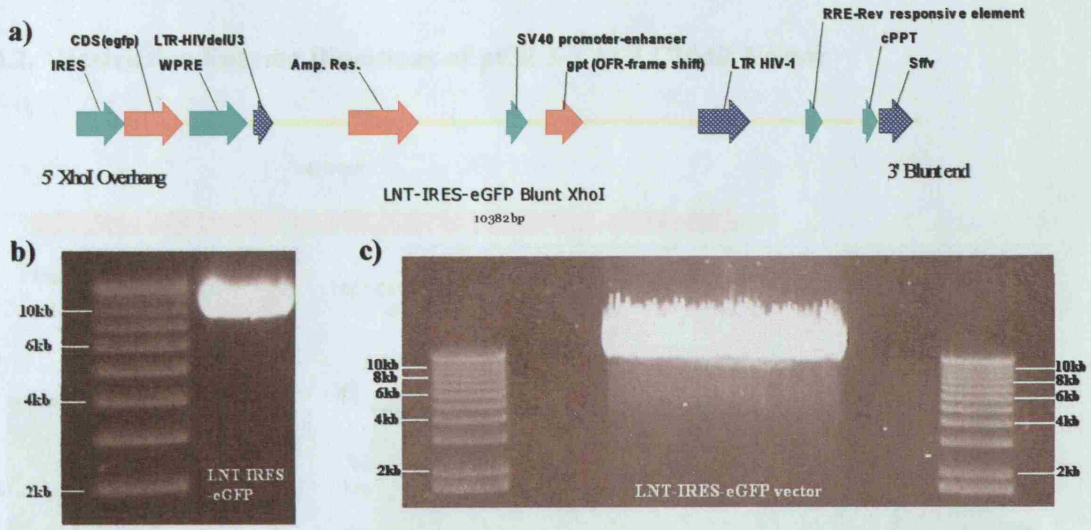

Figure 3.7. Schematic diagram of lentiviral vector plasmid and restriction enzyme digests gel pictures **a)** linear LNT-IRES-eGFP vector with 5'overhang created by XhoI and 3'blunt end; with vector components shown. The digested vector is of 10382 base pair long. **b)** Gel showing first digests of lentiviral vector with BamHI and blunted at about 10kb position **c)** Gel showing second digest of LNT-IRES-eGFP vector with XhoI at approximately 10kb position

Lentiviral vector containing the expression cassette, where TACI gene will be cloned in between SFFV internal promoter and the IRES component, was digested and blunted to produce the final linear form shown in **Figure 3.7a.** First digestion of LNT-IRES-eGFP vector plasmid with BamHI restriction enzyme and followed by blunting of overhangs would expect to produce a 10433 bp fragment; the observed fragment (**Figure 3.7b**) size

resolved on a gel was approximately 10kb. The second digestion with XhoI cut the linear fragment into two fragments, expecting: a 10382bp and a 51bp fragment. **Figure 3.7c** only shows the final linear vector corresponding to approximately 10kb in size.

3.3.2. Restriction Enzyme Digestions of pCR 3-TACI C104R Vector

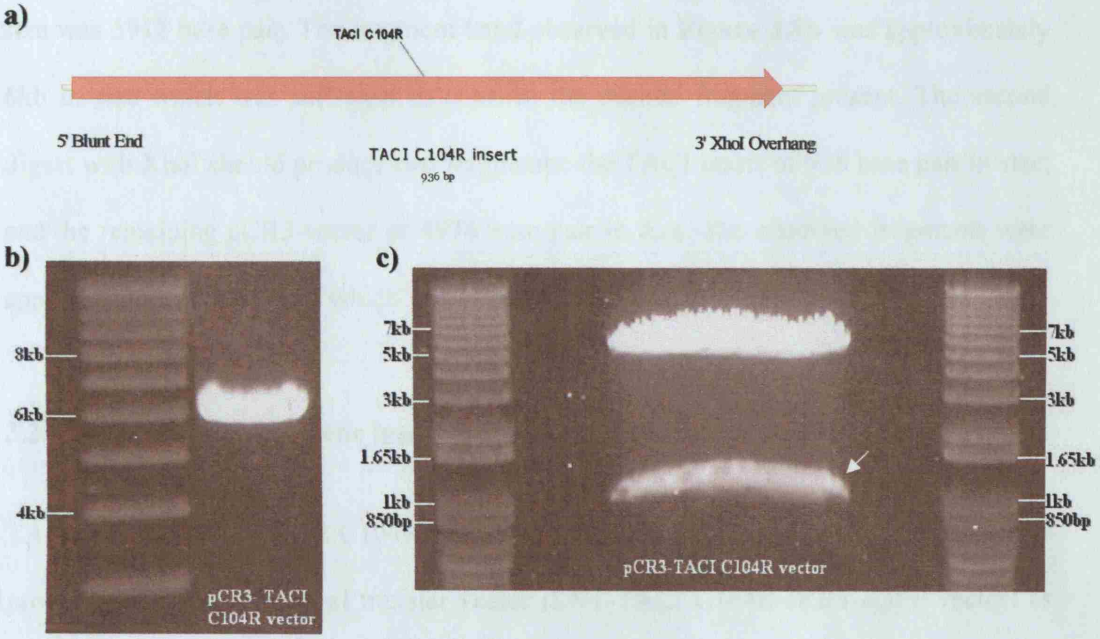

Figure 3.8. Schematic diagram of TACI C104R insert fragment and restriction enzyme digestions of pCR3-TACI C104R vector gel pictures **a)** final TACI gene insert containing the C104R mutation is expected to be 936 base pair long, with 5' blunt end and 3' overhang created by XhoI digestion **b)** Gel picture showing the first digest of the pCR3-TACI C104R with HindIII followed by blunting of overhangs **c)** Gel picture showing the second digest of the linear pCR3-TACI C104R with XhoI producing two fragments. Arrow indicates the band corresponding to the separated TACI gene insert.

The pCR3-TACI C104R was digested to cut out TACI gene and separated from the rest of the vector fragments. The expected TACI insert containing the C104R mutation is of 936bp long as shown in **Figure 3.8**. The gel picture of first digest followed by blunting should produce a linear form of the pCR3-TACI C104R vector; the expected fragment size was 5912 base pair. The fragment band observed in **Figure 3.8b** was approximately 6kb in size which was sufficient to confirm the desired fragment present. The second digest with XhoI should produce two fragments: the TACI insert of 936 base pair in size; and the remaining pCR3 vector of 4976 base pair in size. The observed fragments were approximately 1kb and 5kb which was as expected.

3.3.3. Cloning of TACI gene insert containing C104R mutation into lentiviral vector

TACI insert containing the C104R mutation was cloned into the linear lentiviral vector producing the final lentiviral transfer vector (LNT-TACI C104R-IRES-eGFP vector) as illustrated in **Figure 3.9**. This map represents the final transfer vector if cloning was successful; it also shows the positions of restriction sites. Using the information on the map, the expected number and sizes of fragments when digesting the vector with a particular restriction enzyme were calculated and shown in **Table 3.3.** Plasmid preparations from colonies of transformed cells were then tested for the presence of LNT-TACI C104R-IRES-eGFP vector by digesting it with the following restriction enzymes: ApaI, EcoRI, NotI, SapI and KpnI. The digested fragments were then resolved on a gel and their observed fragment sizes were compared to their respective expected fragment sizes to confirm the presence of TACI gene cloned into the lentiviral vector.

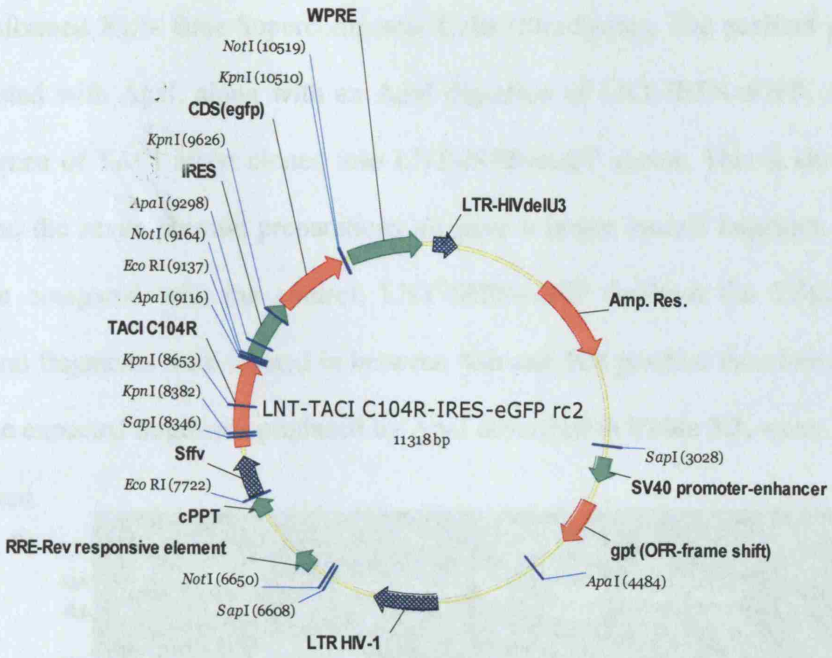

Figure 3.9. Circular map of LNT-TACI C104R-IRES-eGFP vector. TACI insert was cloned in between Sffv internal promoter and IRES element. The map also indicates the positions of restriction sites which are used to calculate fragment sizes when the vector is digested with a particular restriction enzyme. Restriction sites shown includes: ApaI, EcoRI, NotI, SapI and KpnI. The plasmid is 11318 base pairs long.

	ApaI	EcoRI	NotI	SapI	KpnI
Expected no. of fragments produced	3	2	3	3	4
Size of fragment 1 (bp)	6504	9903	7449	6000	9190
Size of fragment 2 (bp)	4632	1415	2514	3580	973
Size of fragment 3 (bp)	182	-	1355	1738	884
Size of fragment 4 (bp)	-	-	-	-	271

Table 3.3. Restriction enzyme reactions that can be performed on LNT-TACI C104R-IRES-eGFP vector plasmid. The expected number of fragments and their sizes produced by each reaction are shown.

Seven plasmid preparations were made from seven different colonies of transformed XL1- Blue Supercompetent Cells (Stratagene). The purified plasmids were digested with ApaI, along with an ApaI digestion of LNT-IRES-eGFP, to confirm the presence of TACI insert cloned into LNT-IRES-eGFP vector. This is shown in **Figure 3.10a,** the seven plasmid preparations all have a larger second fragment, from the top, when compared with the control, LNT-IRES-eGFP (without the TACI insert). The second fragments were located in between 4kb and 5kb position therefore corresponding to the expected fragments produced by ApaI described in **Table 3.3,** when TACI insert is present.

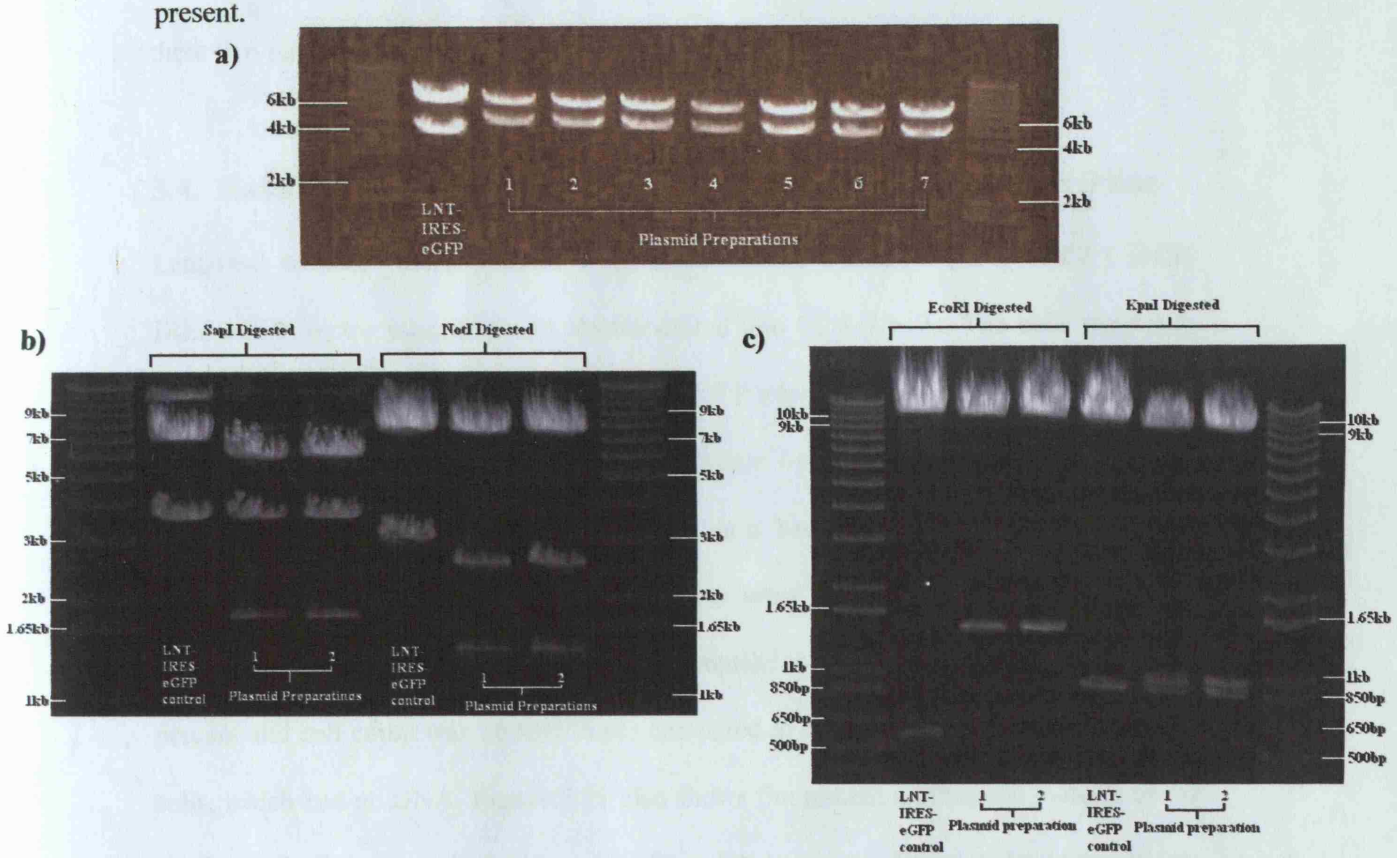

Figure 3.10. Digestions of plasmid preparations, testing for the presence of TACI insert. **a)** digestions with ApaI on 7 different plasmid preparations and on one backbone only control (LNT-IRES-eGFP) **b)** digestions with SapI and NotI on 2 of the 7 plasmid preparations and on a backbone vector control **c)** digestions with EcoRI and KpnI on 2 plasmid preparations and on a backbone vector control.

Two out of the seven plasmid preparations were chosen to be tested with more restriction enzymes: NotI, SapI, EcoRI and KpnI. In **Figure 3.10b**, digestion of plasmid preparation 1 and 2, with SapI restriction enzyme, resulted in 3 fragments produced as expected. The smallest fragments observed were approximately 1.7kb which was similar to the expected fragment calculated in **Table 3.3**. Careful comparison of the sizes of the observed fragments resolved on the gels with the expected sizes of the corresponding fragments described above, confirmed that TACI insert were present in these two plasmid preparations.

3.4. Enhanced green fluorescent protein expression in COS-7 cell line

Lentiviral transfer vector plasmid with TACI C104R transgene (LNT-TACI C104R-IRES-eGFP vector plasmid) were electroporated into COS-7 cells. The cells were then viewed under a fluorescent microscope and eGFP expression was detected as shown in **Figure 3.11d;** cells expressing eGFP are indicated by arrows. COS-7 cells expressing eGFP were also expressing TACI transgene this is because transcription of both eGFP and TACI (C104R) gene were driven by the same internal promoter, spleen focus forming virus (sffv) promoter. The plasmid uptake percentage was approximately 50 percent and cell count was 10 fold lower compared to the electroporation control COS-7 cells, which had no DNA. **Figure 3.11** also shows fluorescent microscope pictures of the control cells that were electroporated with no DNA present; lentiviral backbone vector (LNT-IRES-eGFP) electroporated cells; and lentiviral vector plasmid with wildtype TACI transgene (LNT-TACI-IRES-eGFP vector made by Sylvie Buckridge). All show eGFP expression except the control cells.

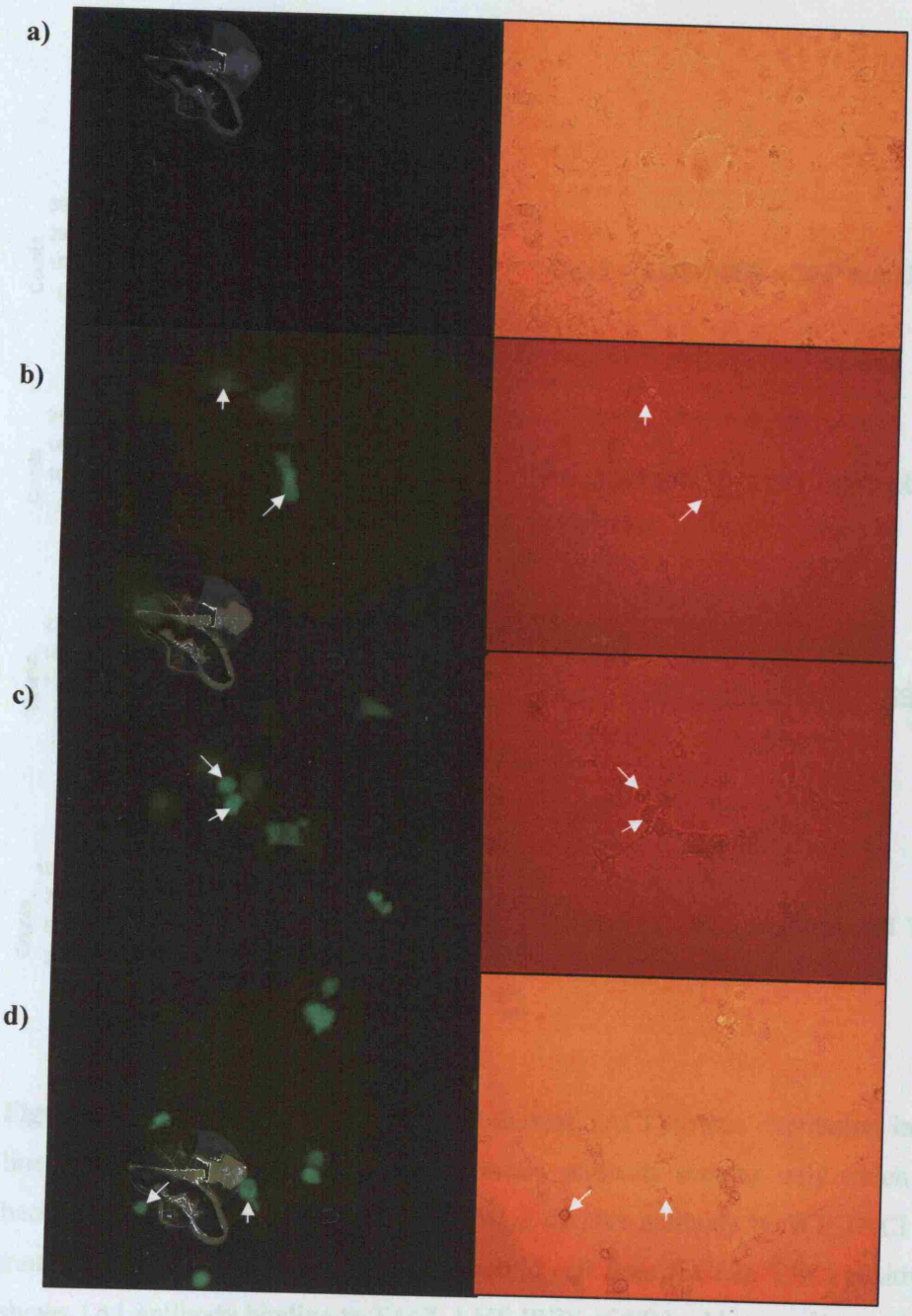

Figure 3.11. Pictures taken under fluorescent microscope; green fluorescence seen in the pictures on the left hand column represents eGFP expression; right hand column shows the exact field but in light phase showing the locations of COS-7 cells. Arrows are for comparison of the eGFP expression and its corresponding cell expressing it. **a)** control cells electroporated with no DNA **b)** cells electroporated with lentiviral backbone vector (LNT-IRES-eGFP) **c)** cells electroporated with lentiviral vector with wildtype TACI transgene (LNT-TACI-IRES-eGFP) **d)** cells electroporated with lentiviral vector with TACI C104R (LNT-TACI C104R-IRES-eGFP vector)

3.5. FACS analysis of wildtype and C104R mutant TACI surface expression in COS-7 cells

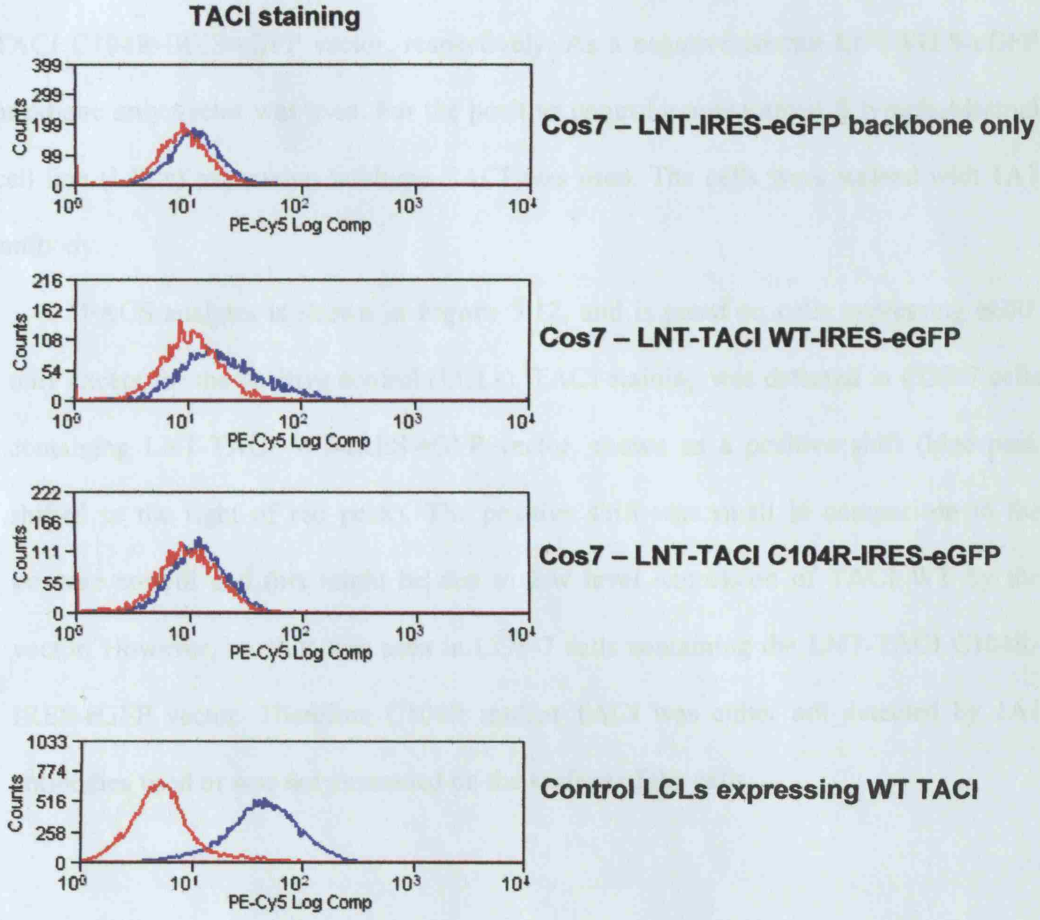

Figure 3.12. Wildtype TACI or C104R mutant TACI surface expression in Cos7 cell lines was tested. Red line indicates secondary antibody staining only which represents background signal; Blue lines show staining of 1A1 antibody to WT TACI or C104R mutant TACI. Transformed B lymphoblastoid cell lines (LCLs), TACI positive control, shows 1A1 antibody binding to TACI. LNT-IRES-eGFP backbone only was the negative control showing no TACI staining. Positive shift in population was shown in Cos7 cells transduced with LNT-TACI WT-IRES-eGFP vector but not cells with LNT-TACI C104R-IRES-eGFP vector.

FACS analysis was performed to test for wildtype TACI or C104R mutant TACI expression in COS-7 cell lines containing either LNT-TACI WT-IRES-eGFP or LNT-TACI C104R-IRES-eGFP vector, respectively. As a negative control LNT-IRES-eGFP backbone only vector was used. For the positive control a transformed B lymphoblastoid cell line (LCLs) expressing wildtype TACI was used. The cells were stained with 1A1 antibody.

FACS analysis is shown in **Figure 3.12,** and is gated on cells expressing eGFP only except for the positive control (LCLs). TACI staining was detected in COS-7 cells containing LNT-TACI WT-IRES-eGFP vector, shown as a positive shift (blue peak shifted to the right of red peak). The positive shift was small in comparison to the positive control and this might be due to low level expression of TACI WT by the vector. However, no shift was seen in COS-7 cells containing the LNT-TACI C104R-IRES-eGFP vector. Therefore C104R mutant TACI was either not detected by 1A1 antibodies used or was not expressed on the surface of the cells.

4. Discussion

4.1. Mutation Screening Strategy

Using the MegaBACE 1000, a multiplex capillary heteroduplex analysis technique, high throughput of HA carried out on a large number of patients and on several different fragments of interests was possible. Samples screened positive for sequence alteration in HA were then subsequently sequenced to identify the exact mutation. This system is simple to set up, requires little experience to perform, less expensive than direct sequencing and saves time. However, the ability of HA to detect certain mismatches are influenced by other factors (Hoskins, Thorn, Scambler, & Beales 2003). TACI gene exon 4 was more difficult to screen for mutations in comparison with exon 3. The HA of changes found in exon 4 have very subtle difference morphology to the HA of wildtype TACI exon 4. In order to maintain sensitivity in detecting mutations in exon 4, caution was taken whilst selecting samples for direct sequencing. A total of 8 samples were suspected to have potential sequence alterations based on their HA and only 1 out of the 8 samples were confirmed with a mutation. Consequently the HA of TACI exon 4 fragments resulted in an increased number of 'false positive' samples. In contrast, mutations found in TACI exon 3 had distinct HA patterns, easily identifiable, unlike TACI exon 4. As a result a smaller sample number were chosen, based on their HA, for sequencing whilst maintaining the sensitivity of the system.

4.2. TACI gene mutations identified in CVID patients

4.2.1. C104R mutation in TACI

C104R representing amino acid substitution of cysteine 104 with arginine is caused by a missense mutation of nucleotide position 310 thymine (T) to cytosine (C) substitution (c.310T>C) in TACI exon 3. High frequency of heterozygous C104R TACI mutation was found, in 2 out of 26 CVID patients. When compared with the frequency of C104R in 47 healthy controls none were found. Therefore, this suggests frequency of C104R mutations in TACI are increased in CVID cases. To examine whether C104R mutation is associated with CVID one would look at the segregation pattern of both the mutation (C104R) and CVID in a multiplex family- more than one family member affected by the immunodeficiency. Due to lack of familial data of patient RH02 and RH04 analysis of segregation within their family was not performed. C104R mutation was observed in families with multiple CVID cases in previous studies (Castigli, Wilson, Garibyan, Rachid, Bonilla, Schneider, & Geha 2005;Salzer, Chapel, Webster, Pan-Hammarstrom, Schmitt-Graeff, Schlesier, Peter, Rockstroh, Schneider, Schaffer, Hammarstrom, & Grimbacher 2005). Pattern of inheritance, serum immunoglobulin levels and presence of CVID phenotypes were determined in these families. In all the families C104R mutation co-segregated with CVID therefore the mutation is disease associated.

C104R substitution is found in the cysteine rich domain 2 (aa 68 to 106) of the extracellular domain of TACI, where the affected cysteine residue is conserved. The substitution could potentially disrupt structurally important disulfide bond formed between cysteine 104 and cysteine 93, therefore possibly abolishing ligand binding site

for BAFF and APRIL (Salzer, Chapel, Webster, Pan-Hammarstrom, Schmitt-Graeff, Schlesier, Peter, Rockstroh, Schneider, Schaffer, Hammarstrom, & Grimbacher 2005).

The serum IgG level of patient RH02 and RH04, carrying heterozygous C104R, were measured at the time of diagnosis. Their IgG levels, 10 g l^{-1} and 9.3 g l^{-1} respectively, were within the normal range (7 – 16 g l^{-1}). In contrast their serum IgA (0.1 and 0.3; normal range is 0.7- 4.0g l^{-1}) and serum IgM (0.1 and 0.2; normal range is 0.4-2.3g l^{-1}) at the time of diagnosis were reduced. This can be explained by the BAFF-APRIL system and its affected receptors. APRIL mediates class switch recombination of IgG and IgA through TACI; BAFF mediates IgG secretion also through TACI but BAFFR as well. TACI defect such as C104R would lead to impaired IgA secretion but not IgG secretion as this is mediated via BAFF-BAFFR interaction. On the contrary, CVID patients carrying the same C104R mutation in the previous study of Salzer et al, had severely lowered IgA and IgG secretion (Salzer, Chapel, Webster, Pan-Hammarstrom, Schmitt-Graeff, Schlesier, Peter, Rockstroh, Schneider, Schaffer, Hammarstrom, & Grimbacher 2005). They postulated that TACI plays an essential role in mediating BAFF and APRIL induced CSR of both IgA and IgG in human, even with normal BAFFR functions. This was different to the phenotype observed in TACI null mice which had impaired IgA and IgM secretion only and normal IgG levels (von Bulow, van Deursen, & Bram 2001). This maybe due to inherent differences between murine and human systems.

The ability of defective TACI binding to APRIL and BAFF was shown to be abolished in heterologous cell lines expressing TACI with C104R homozygous mutation; this explains the impaired proliferative response to IgM-APRIL stimulation and

defective induction of class-switch recombination of IgA and IgG (Salzer, Chapel, Webster, Pan-Hammarstrom, Schmitt-Graeff, Schlesier, Peter, Rockstroh, Schneider, Schaffer, Hammarstrom, & Grimbacher 2005). However, APRIL binding in patients peripheral B cells heterozygous for this mutation was not affected suggesting normal trimerisation of only normal TACI forming functional signaling complexes excluding the incorporation of mutant TACI. Therefore this raises the question of how heterozygous TACI mutations lead to disease phenotype.

To conclude the evidence thus far suggests that C104R is a significant mutation towards the pathogenesis of TACI deficiency and possibly involved in CVID. The experiments demonstrated the abolished binding of APRIL and BAFF with TACI containing a homozygous C104R change showing that the conserved cysteine 104 in CRD2 is essential in ligand-receptor interaction and TACI function. However, ligand-receptor binding was not affected in heterozygous C104R mutant TACI suggesting normal TACI functions. But this is not the case; individuals carrying a heterozygous C104R mutation in TACI have impaired IgG and IgA secretion in response to APRIL and BAFF stimulation (Castigli, Wilson, Garibyan, Rachid, Bonilla, Schneider, & Geha 2005). It is therefore important to establish the missing pathogenic mechanism of heterozygous C104R mutation in TACI, linking the defective ligand binding of some, but not all, TACI receptors expressed on B cells surface and their impaired responses towards APRIL and BAFF ligand stimulation. A potential experiment to investigate this would be to examine how heterozygous C104R mutation in TACI affect downstream signaling pathway such as NF-κB and NF-AT in highly purified B cells of patients or a an equivalent heterologous B cell line model. This will examine the effect of heterozygous

mutations have on the signaling complexes formed rather than examining individual TACI receptors.

4.2.2. Identification of TACI mutations

An ongoing collaborative effort by the Molecular Immunology Unit (ICH) and groups from the UK (Royal Free Hospital, John Radcliffe Hospital) and Germany (University of Freiburg) have screened 529 CVID patients and found 45 individuals carrying heterozygous, homozygous or compound heterozygous mutations within *TNFRSF13B* encoding TACI (unpublished data). The frequency thus far indicates approximately 8% of CVID patient subgroup carry TACI defect. **Table 4.1** shows 16 different mutations that causes non-conservative changes in the amino acid sequence of TACI.

C104R mutation was found at the greatest frequency; 20 individuals carried heterozygous C104R; 6 were compound heterozygotes; 1 was homozygote for C104R. Compared with the 218 healthy controls screened only 4 heterozygote C104R were found. The increased incidence of C104R mutant TACI in CVID cases, observed here, provides further evidence of the involvement of TACI deficiency in the pathogenesis of immunodeficiencies.

Table 4.1. 45 CVID patients out of 529 were identified with mutations in TACI gene (unpublished data). Homozygous, heterozygous and compound heterozygous mutations were found. Mutations of the same type are colour coded. Frequency of patients with corresponding mutations is shown.

	Change	No. of patients
Homozygotes	C104R	1
Compound heterozygotes	Y79C/I87N	1
	C104R/204InsA	2
	C104R/571InsG	1
	C104R/C104Y	1
	C104R/S144X	1
	C104R/S194X	1
	204InsA/L118P	1
	G152E/A181E	1
	L171R/A181E	1
Heterozygotes	I87N	2
	298InsT	1
	C104R	20
	Y164X	1
	L171R	2
	C172Y	1
	A181E	6
	C193X	1

4.2.3. A181E change in TACI

A181E represents amino acid substitution of alanine 181 with glutamic acid caused by a single nucleotide substitution of 542 cytosine to adenine (A) in exon 4 of TACI gene. Amino acid change is located in the transmembrane domain of TACI proximal to the intracellular domain. In the cohort of CVID patients screened (**Table 4.1**): 2 patients were found with compound heterozygous mutation with one allele containing A181E; and 6 patients that are heterozygote for this change. Despite the high frequency at which A181E is found in CVID population a comparable frequency is observed in control population and there is insufficient evidence of co-segregation of mutant allele with phenotypes within indexed families (L. Hammarstrom, unpublished data). Therefore, missense mutation causing A181E may just be a polymorphism change.

4.2.4. Insertion mutation in TACI

204InsA represents a single adenine insertion immediately following position 204 in exon 3 of TACI gene. This mutation is found in 3 CVID individuals (**Table 4.1**) carrying compound heterozygous mutation, affecting one of the two alleles of the TACI gene; the same mutation was observed in a compound heterozygote in a previous study (Castigli, Wilson, Garibyan, Rachid, Bonilla, Schneider, & Geha 2005). Insertion of adenine causes frameshift after amino acid 68 and causes premature termination of protein at aa 79.

Screening of CVID patients in MIU also identified a new insertion change, 571insG, guanine insertion immediately after base pair position 571 in exon 4 of TACI gene. The resulting TACI protein is truncated and prematurely terminated at amino acid 235. This frame shift mutation disrupts the intracellular domain of TACI and is predicted to abolish both CAML and TRAFs mediated downstream signaling, NF-κB and NF-AT activation.

4.3. Polymorphism or not?

Polymorphism is generally described as the different forms of alleles found at a single genetic locus. Identifying variations in a particular gene, such as TACI, the term polymorphisms apply to variants which are present at frequency greater than, for example, one percent in healthy controls. It can also be applied to variants which are nonpathogenic, non-contributing towards disease phenotype, or have no effect on amino acid sequence. I use the term polymorphism here in both contexts.

T27T, P97P and S277S found in screening of both CVID patients and controls were silent mutations. The nucleotide substituted has no effect on the codon that

encodes for the amino acid sequence. Synonymous changes have no consequences on TACI functions as it does not affect the amino acid sequence therefore are considered as polymorphisms. T27T and S277S changes were also reported in previous studies (Salzer, Chapel, Webster, Pan-Hammarstrom, Schmitt-Graeff, Schlesier, Peter, Rockstroh, Schneider, Schaffer, Hammarstrom, & Grimbacher 2005) as polymorphisms.

R72H and P251L changes are also known polymorphisms described previously by Salzer et al. The changes were non-synonymous, nucleotide substitutions resulting in an amino acid sequence change. However, they were identified as polymorphisms on the basis of the similar frequency level found in healthy controls. In this study R72H was only found in healthy controls.

R202H is an amino acid substitution near transmembrane domain of the intracellular domain of TACI. This was described in two previous studies each describing one CVID patient carrying R202H. (Castigli, Wilson, Garibyan, Rachid, Bonilla, Schneider, & Geha 2005;Salzer, Chapel, Webster, Pan-Hammarstrom, Schmitt-Graeff, Schlesier, Peter, Rockstroh, Schneider, Schaffer, Hammarstrom, & Grimbacher 2005). The proposed cause of TACI defect in patients with R202H was interference with CAML and TRAF interaction effecting downstream signaling and functions. However, R202H was not found on further screening of 529 CVID patients and one R202H heterogzygote was found in healthy controls. In this study one CVID patient and one healthy control carried the R202H change thus providing further evidence that R202H is a polymorphism that occurs at similar frequency in both CVID cases and healthy controls. Using SIFT

One healthy control was found to carry a new rare heterozygous K188M polymorphism. It was only described once in a CVID patient by Uli Salzer but was not

published result. Screening of 529 CVID patients and 218 healthy controls did not identify a single K188M change. This shows how difficult it is to determine the true frequency of a particular mutation, especially with rare variants such as K188M. Therefore, K188M shouldn't be ruled out as a mutation and that the 'healthy' control in which the change was identified could have a mild CVID phenotype. As described before lysine 188 is found right after the transmembrane domain of TACI in the intracellular region but lysine is not conserved in rat or mouse. On performing an analysis on SIFT (sort intolerant from tolerant) program on K188M change, it was predicted to be functionally deleterious (Ng & Henikoff 2003).

4.4. Cloning of C104R mutant TACI gene into a lentiviral transfer vector and expression of mutant TACI in heterologous cell line

The justifications for expressing TACI wild type and TACI mutants in a lentiviral expression system, *in vitro* and *in vivo*, are its benefit over other gene delivery methods. Lentiviral expression system based on the production of viral particles and infection of target cells allow long-term stable expression is lacking in other expression systems. Importantly, using a lentiviral expression system, a heterozygote mutant model can be created to simulate the genetic defect seen in most patients.

The cloning strategy used was very straightforward involving two step of complete digestion of the LNT-IRES-eGFP backbone vector and pCR-3-TACI C104R plasmid. After ligation and transformation of cells the resulting plasmid preparations were all tested positive for the TACI insert, when digested with a variety of restriction enzymes. However, confirmation by direct sequencing of the lentiviral vector with TACI C104R insert will be needed.

The expression of TACI wild-type (LNT-TACI WT-IRES-eGFP vector previously generate) and TACI C104R mutant were then evaluated by electroporation of vectors into a heterologous cell line called COS-7. Expression levels are regulated by the spleen focus forming virus (Sffv) internal promoter. TACI insert and eGFP gene are transcribed simultaneously; but due to the internal ribosome entry site (IRES) sequence located in between TACI and eGFP their mRNA are translated independently resulting in two independent proteins. Therefore, detection of eGFP under fluorescent microscope is a good indication of the presence of both wildtype and mutant TACI expression at the transcriptional and translational level.

Subsequent FACS analysis examines the expression of both wildtype TACI and C104R mutant TACI on the cell surface by staining with monoclonal rat IgG anti-human TACI antibody (1A1 antibody used by Salzer et al.) Significant wild-type TACI surface expression was observed in comparison with backbone vector negative control cells. However, it was unable to detect any significant C104R mutant TACI expression. eGFP expression was observed prior to FACS staining with 1A1 antibody; therefore this may suggest expressed C104R TACI mutants were expressed intracellularly. In contrast a previous study by Salzer et al. mutant C104R TACI was detected on isolated peripheral blood mononuclear cells (PBMCs) using polyclonal TACI antibody. They also tried using the same 1A1 monoclonal antibody to detect mutant TACI but failed; the group eventually mapped the antibody epitope on to a region that is disrupted by the C104R change. Therefore, the expression of C104R mutant TACI was possibly undetected by 1A1 antibody due to the abrogated epitope site.

4.5. Future work

The analysis of larger CVID patient cohort for mutations in TACI will identify the mutations that are important in causing TACI defects in CVID. Through this candidate approach, TACI gene with the various mutations can be cloned into an expression system for further functional analysis and determine how each mutation contributes towards the disease phenotype. Lentiviral expression systems has many named benefits in creating *in vitro* and *in vivo* model, this study shows some preliminary data on the expression levels capable by this system. However, further work to generate the viral particles and the evaluation of the TACI expression levels upon integration into host genome are needed.

References

Agematsu, K., Futatani, T., Hokibara, S., Kobayashi, N., Takamoto, M., Tsukada, S., Suzuki, H., Koyasu, S., Miyawaki, T., Sugane, K., Komiyama, A., & Ochs, H. D. 2002, "Absence of memory B cells in patients with common variable immunodeficiency", *Clin.Immunol.*, vol. 103, no. 1, pp. 34-42.

Ashman, R. F., Schaffer, F. M., Kemp, J. D., Yokoyama, W. M., Zhu, Z. B., Cooper, M. D., & Volanakis, J. E. 1992, "Genetic and immunologic analysis of a family containing five patients with common-variable immune deficiency or selective IgA deficiency", *J Clin.Immunol.*, vol. 12, no. 6, pp. 406-414.

Beier, K. C., Hutloff, A., Dittrich, A. M., Heuck, C., Rauch, A., Buchner, K., Ludewig, B., Ochs, H. D., Mages, H. W., & Kroczek, R. A. 2000, "Induction, binding specificity and function of human ICOS", *Eur.J Immunol.*, vol. 30, no. 12, pp. 3707-3717.

Bhattacharyya, A. & Lilley, D. M. 1989, "The contrasting structures of mismatched DNA sequences containing looped-out bases (bulges) and multiple mismatches (bubbles)", *Nucleic Acids Res.*, vol. 17, no. 17, pp. 6821-6840.

Blesch, A. 2004, "Lentiviral and MLV based retroviral vectors for ex vivo and in vivo gene transfer", *Methods*, vol. 33, no. 2, pp. 164-172.

Bodmer, J. L., Schneider, P., & Tschopp, J. 2002, "The molecular architecture of the TNF superfamily", *Trends Biochem.Sci.*, vol. 27, no. 1, pp. 19-26.

Bryant, A., Calver, N. C., Toubi, E., Webster, A. D., & Farrant, J. 1990, "Classification of patients with common variable immunodeficiency by B cell secretion of IgM and IgG in response to anti-IgM and interleukin-2", *Clin.Immunol.Immunopathol.*, vol. 56, no. 2, pp. 239-248.

Castigli, E. & Geha, R. S. 2006, "Molecular basis of common variable immunodeficiency", *J Allergy Clin.Immunol.*, vol. 117, no. 4, pp. 740-746.

Castigli, E., Wilson, S. A., Garibyan, L., Rachid, R., Bonilla, F., Schneider, L., & Geha, R. S. 2005, "TACI is mutant in common variable immunodeficiency and IgA deficiency", *Nat.Genet.*, vol. 37, no. 8, pp. 829-834.

Cunningham-Rundles, C. & Bodian, C. 1999, "Common variable immunodeficiency: clinical and immunological features of 248 patients", *Clin.Immunol.*, vol. 92, no. 1, pp. 34-48.

Day, E. S., Cachero, T. G., Qian, F., Sun, Y., Wen, D., Pelletier, M., Hsu, Y. M., & Whitty, A. 2005, "Selectivity of BAFF/BLyS and APRIL for binding to the TNF family receptors BAFFR/BR3 and BCMA", *Biochemistry*, vol. 44, no. 6, pp. 1919-1931.

Den Dunnen, J. T. & Van Ommen, G. J. 1999, "The protein truncation test: A review", *Hum.Mutat.*, vol. 14, no. 2, pp. 95-102.

Don, R. H., Cox, P. T., Wainwright, B. J., Baker, K., & Mattick, J. S. 1991, 'Touchdown' PCR to circumvent spurious priming during gene amplification", *Nucleic Acids Research.*, vol. 19, no. 14, pp. 4-4.

Donello, J. E., Loeb, J. E., & Hope, T. J. 1998, "Woodchuck hepatitis virus contains a tripartite posttranscriptional regulatory element", *J Virol.*, vol. 72, no. 6, pp. 5085-5092.

Engel, P., Zhou, L. J., Ord, D. C., Sato, S., Koller, B., & Tedder, T. F. 1995, "Abnormal B lymphocyte development, activation, and differentiation in mice that lack or overexpress the CD19 signal transduction molecule", *Immunity.*, vol. 3, no. 1, pp. 39-50.

Espanol, T., Catala, M., Hernandez, M., Caragol, I., & Bertran, J. M. 1996, "Development of a common variable immunodeficiency in IgA-deficient patients", *Clin.Immunol.Immunopathol.*, vol. 80, no. 3 Pt 1, pp. 333-335.

Fearon, D. T. & Carroll, M. C. 2000, "Regulation of B lymphocyte responses to foreign and self-antigens by the CD19/CD21 complex", *Annu.Rev.Immunol.*, vol. 18, pp. 393-422.

Foy, T. M., Aruffo, A., Bajorath, J., Buhlmann, J. E., & Noelle, R. J. 1996, "Immune regulation by CD40 and its ligand GP39", *Annu.Rev.Immunol.*, vol. 14, pp. 591-617.

Goldacker, S. & Warnatz, K. 2005, "Tackling the heterogeneity of CVID", *Curr.Opin.Allergy Clin.Immunol.*, vol. 5, no. 6, pp. 504-509.

Grimbacher, B., Hutloff, A., Schlesier, M., Glocker, E., Warnatz, K., Drager, R., Eibel, H., Fischer, B., Schaffer, A. A., Mages, H. W., Kroczek, R. A., & Peter, H. H. 2003, "Homozygous loss of ICOS is associated with adult-onset common variable immunodeficiency", *Nat.Immunol.*, vol. 4, no. 3, pp. 261-268.

Hayes, V. M., Wu, Y., Osinga, J., Mulder, I. M., van, d., V, Elfferich, P., Buys, C. H., & Hofstra, R. M. 1999, "Improvements in gel composition and electrophoretic conditions for broad-range mutation analysis by denaturing gradient gel electrophoresis", *Nucleic Acids Res.*, vol. 27, no. 20, p. e29.

Highsmith, W. E., Jr., Nataraj, A. J., Jin, Q., O'Connor, J. M., El-Nabi, S. H., Kusukawa, N., & Garner, M. M. 1999, "Use of DNA toolbox for the characterization of mutation scanning methods. II: evaluation of single-strand conformation polymorphism analysis", *Electrophoresis*, vol. 20, no. 6, pp. 1195-1203.

Hoskins, B. E., Thorn, A., Scambler, P. J., & Beales, P. L. 2003, "Evaluation of multiplex capillary heteroduplex analysis: a rapid and sensitive mutation screening technique", *Hum.Mutat.*, vol. 22, no. 2, pp. 151-157.

Hutloff, A., Dittrich, A. M., Beier, K. C., Eljaschewitsch, B., Kraft, R., Anagnostopoulos, I., & Kroczek, R. A. 1999, "ICOS is an inducible T-cell co-stimulator structurally and functionally related to CD28", *Nature*, vol. 397, no. 6716, pp. 263-266.

Hymowitz, S. G., Patel, D. R., Wallweber, H. J., Runyon, S., Yan, M., Yin, J., Shriver, S. K., Gordon, N. C., Pan, B., Skelton, N. J., Kelley, R. F., & Starovasnik, M. A. 2005, "Structures of APRIL-receptor complexes: like BCMA, TACI employs only a single cysteine-rich domain for high affinity ligand binding", *J Biol.Chem.*, vol. 280, no. 8, pp. 7218-7227.

Kim, V. N., Mitrophanous, K., Kingsman, S. M., & Kingsman, A. J. 1998, "Minimal requirement for a lentivirus vector based on human immunodeficiency virus type 1", *J Virol.*, vol. 72, no. 1, pp. 811-816.

Lambrinakos, A., Humphrey, K. E., Babon, J. J., Ellis, T. P., & Cotton, R. G. 1999, "Reactivity of potassium permanganate and tetraethylammonium chloride with mismatched bases and a simple mutation detection protocol", *Nucleic Acids Res.*, vol. 27, no. 8, pp. 1866-1874.

Litinskiy, M. B., Nardelli, B., Hilbert, D. M., He, B., Schaffer, A., Casali, P., & Cerutti, A. 2002, "DCs induce CD40-independent immunoglobulin class switching through BLyS and APRIL", *Nat.Immunol.*, vol. 3, no. 9, pp. 822-829.

Liu, W., Smith, D. I., Rechtzigel, K. J., Thibodeau, S. N., & James, C. D. 1998, "Denaturing high performance liquid chromatography (DHPLC) used in the detection of germline and somatic mutations", *Nucleic Acids Res.*, vol. 26, no. 6, pp. 1396-1400.

Lopez-Fraga, M., Fernandez, R., Albar, J. P., & Hahne, M. 2001, "Biologically active APRIL is secreted following intracellular processing in the Golgi apparatus by furin convertase", *EMBO Rep.*, vol. 2, no. 10, pp. 945-951.

Mackay, F., Schneider, P., Rennert, P., & Browning, J. 2003, "BAFF AND APRIL: a tutorial on B cell survival", *Annu.Rev.Immunol.*, vol. 21, pp. 231-264.

Manning, W. C., Murphy, J. E., Jolly, D. J., Mento, S. J., & Ralston, R. O. 1998, "Use of a recombinant murine cytomegalovirus expressing vesicular stomatitis virus G protein to pseudotype retroviral vectors", *J Virol.Methods*, vol. 73, no. 1, pp. 31-39.

Miyoshi, H., Blomer, U., Takahashi, M., Gage, F. H., & Verma, I. M. 1998, "Development of a self-inactivating lentivirus vector", *J Virol.*, vol. 72, no. 10, pp. 8150-8157.

Ng, P. C. & Henikoff, S. 2003, "SIFT: Predicting amino acid changes that affect protein function", *Nucleic Acids Res.*, vol. 31, no. 13, pp. 3812-3814.

Piqueras, B., Lavenu-Bombled, C., Galicier, L., Bergeron-van der, C. F., Mouthon, L., Chevret, S., Debre, P., Schmitt, C., & Oksenhendler, E. 2003, "Common variable

immunodeficiency patient classification based on impaired B cell memory differentiation correlates with clinical aspects", *J Clin.Immunol.*, vol. 23, no. 5, pp. 385-400.

Rickert, R. C., Rajewsky, K., & Roes, J. 1995, "Impairment of T-cell-dependent B-cell responses and B-1 cell development in CD19-deficient mice", *Nature*, vol. 376, no. 6538, pp. 352-355.

Salzer, U., Chapel, H. M., Webster, A. D., Pan-Hammarstrom, Q., Schmitt-Graeff, A., Schlesier, M., Peter, H. H., Rockstroh, J. K., Schneider, P., Schaffer, A. A., Hammarstrom, L., & Grimbacher, B. 2005, "Mutations in TNFRSF13B encoding TACI are associated with common variable immunodeficiency in humans", *Nat.Genet.*, vol. 37, no. 8, pp. 820-828.

Salzer, U. & Grimbacher, B. 2005, "TACItly changing tunes: farewell to a yin and yang of BAFF receptor and TACI in humoral immunity? New genetic defects in common variable immunodeficiency", *Curr.Opin.Allergy Clin.Immunol.*, vol. 5, no. 6, pp. 496-503.

Salzer, U., Maul-Pavicic, A., Cunningham-Rundles, C., Urschel, S., Belohradsky, B. H., Litzman, J., Holm, A., Franco, J. L., Plebani, A., Hammarstrom, L., Skrabl, A., Schwinger, W., & Grimbacher, B. 2004, "ICOS deficiency in patients with common variable immunodeficiency", *Clin.Immunol.*, vol. 113, no. 3, pp. 234-240.

Schneider, P. 2005, "The role of APRIL and BAFF in lymphocyte activation", *Curr.Opin.Immunol.*, vol. 17, no. 3, pp. 282-289.

Seshasayee, D., Valdez, P., Yan, M., Dixit, V. M., Tumas, D., & Grewal, I. S. 2003, "Loss of TACI causes fatal lymphoproliferation and autoimmunity, establishing TACI as an inhibitory BLyS receptor", *Immunity.*, vol. 18, no. 2, pp. 279-288.

Thompson, J. S., Bixler, S. A., Qian, F., Vora, K., Scott, M. L., Cachero, T. G., Hession, C., Schneider, P., Sizing, I. D., Mullen, C., Strauch, K., Zafari, M., Benjamin, C. D., Tschopp, J., Browning, J. L., & Ambrose, C. 2001, "BAFF-R, a newly identified TNF receptor that specifically interacts with BAFF", *Science*, vol. 293, no. 5537, pp. 2108-2111.

van Zelm, M. C., Reisli, I., van der, B. M., Castano, D., van Noesel, C. J., van Tol, M. J., Woellner, C., Grimbacher, B., Patino, P. J., van Dongen, J. J., & Franco, J. L. 2006, "An antibody-deficiency syndrome due to mutations in the CD19 gene", *N.Engl.J.Med.*, vol. 354, no. 18, pp. 1901-1912.

Vigna, E. & Naldini, L. 2000, "Lentiviral vectors: excellent tools for experimental gene transfer and promising candidates for gene therapy", *J Gene Med*, vol. 2, no. 5, pp. 308-316.

von Bulow, G. U. & Bram, R. J. 1997, "NF-AT activation induced by a CAML-interacting member of the tumor necrosis factor receptor superfamily", *Science*, vol. 278, no. 5335, pp. 138-141.

von Bulow, G. U., van Deursen, J. M., & Bram, R. J. 2001, "Regulation of the T-independent humoral response by TACI", *Immunity.*, vol. 14, no. 5, pp. 573-582.

Vorechovsky, I., Cullen, M., Carrington, M., Hammarstrom, L., & Webster, A. D. 2000, "Fine mapping of IGAD1 in IgA deficiency and common variable immunodeficiency: identification and characterization of haplotypes shared by affected members of 101 multiple-case families", *J Immunol.*, vol. 164, no. 8, pp. 4408-4416.

Warnatz, K., Denz, A., Drager, R., Braun, M., Groth, C., Wolff-Vorbeck, G., Eibel, H., Schlesier, M., & Peter, H. H. 2002, "Severe deficiency of switched memory B cells (CD27(+)IgM(-)IgD(-)) in subgroups of patients with common variable immunodeficiency: a new approach to classify a heterogeneous disease", *Blood*, vol. 99, no. 5, pp. 1544-1551.

Xia, X. Z., Treanor, J., Senaldi, G., Khare, S. D., Boone, T., Kelley, M., Theill, L. E., Colombero, A., Solovyev, I., Lee, F., McCabe, S., Elliott, R., Miner, K., Hawkins, N., Guo, J., Stolina, M., Yu, G., Wang, J., Delaney, J., Meng, S. Y., Boyle, W. J., & Hsu, H. 2000, "TACI is a TRAF-interacting receptor for TALL-1, a tumor necrosis factor family member involved in B cell regulation", *J Exp.Med*, vol. 192, no. 1, pp. 137-143.

Yan, M., Wang, H., Chan, B., Roose-Girma, M., Erickson, S., Baker, T., Tumas, D., Grewal, I. S., & Dixit, V. M. 2001, "Activation and accumulation of B cells in TACI-deficient mice", *Nat.Immunol.*, vol. 2, no. 7, pp. 638-643.

Yoshinaga, S. K., Whoriskey, J. S., Khare, S. D., Sarmiento, U., Guo, J., Horan, T., Shih, G., Zhang, M., Coccia, M. A., Kohno, T., Tafuri-Bladt, A., Brankow, D., Campbell, P., Chang, D., Chiu, L., Dai, T., Duncan, G., Elliott, G. S., Hui, A., McCabe, S. M., Scully, S., Shahinian, A., Shaklee, C. L., Van, G., Mak, T. W., & Senaldi, G. 1999, "T-cell co-stimulation through B7RP-1 and ICOS", *Nature*, vol. 402, no. 6763, pp. 827-832.

Appendix A – Heteroduplex Analysis and Direct Seqencing of 26 CVID patients

Exon 1

Sample No.	HA prediction	Sequencing Conclusion	Sequenced?
RH01	possible change	wt	yes
RH02	possible change	wt	yes
RH03	possible change	wt	yes
RH04	wt		no
RH05	wt		no
RH06	wt		no
RH07	inconclusive	inconclusive	yes
RH08	wt		no
RH09	possible change	inconclusive	yes
RH10	possible change	wt	yes
RH11	wt		no
RH12	wt		no
RH13	possible change	wt	yes
RH14	wt		no
RH15	inconclusive	inconclusive	yes
RH16	wt		no
RH17	wt		no
RH18	wt		no
RH19	possible change	wt	yes
RH20	wt		no
RH21	wt		no
RH22	possible change	inconclusive	yes
RH23	possible change	wt	yes
RH24	possible change	wt	yes
RH25	possible change	inconclusive	yes
RH26	possible change	wt	yes

Exon 2

Sample No.	HA prediction	Sequencing Conclusion	Sequenced?
RH01	inconclusive		no
RH02	homozygous SNP		no
RH03	heterozygous SNP		no
RH04	heterozygous SNP		no
RH05	heterozygous SNP		no
RH06	homozygous SNP		no
RH07	heterozygous SNP		no
RH08	homozygous SNP		no
RH09	wt		no
RH10	homozygous SNP		no
RH11	wt		no
RH12	homozygous SNP		no
RH13	wt		no
RH14	heterozygous SNP		no

RH15	inconclusive		no
RH16	heterozygous SNP		no
RH17	homozygous SNP		no
RH18	homozygous SNP		no
RH19	homozygous SNP		no
RH20	heterozygous SNP		no
RH21	homozygous SNP		no
RH22	heterozygous SNP		no
RH23	heterozygous SNP		no
RH24	wt		no
RH25	heterozygous SNP		no
RH26	homozygous SNP		no

Exon 3

Sample No.	HA prediction	Sequencing Conclusion	Sequenced?
RH01	Heterozygous SNP		no
RH02	Heterozygous C104R	C104R	yes
RH03	wt		no
RH04	Heterozygous C104R + SNP	C104R + SNP	yes
RH05	Heterozygous SNP		no
RH06	Heterozygous SNP		no
RH07	possible change	SNP	yes
RH08	wt		no
RH09	wt		no
RH10	wt		no
RH11	wt		no
RH12	wt		no
RH13	wt		no
RH14	wt		no
RH15	wt		no
RH16	Heterozygous SNP		no
RH17	wt		no
RH18	wt		no
RH19	wt		no
RH20	Heterozygous SNP		no
RH21	wt		no
RH22	Heterozygous SNP		no
RH23	Heterozygous SNP		no
RH24	Homozygous SNP		no
RH25	Heterozygous SNP		no
RH26	wt		no

Exon 4

Sample No.	HA prediction	Sequencing Conclusion	Sequenced?
RH01	possible change	wt	yes
RH02	possible change	wt	yes
RH03	wt		no

RH04	wt		no
RH05	wt		no
RH06	wt		no
RH07	wt		no
RH08	wt		no
RH09	wt		no
RH10	wt		no
RH11	wt		no
RH12	possible change	wt	yes
RH13	possible change	R202H	yes
RH14	wt		no
RH15	wt		no
RH16	possible change	wt	yes
RH17	wt		no
RH18	wt		no
RH19	possible change	wt	yes
RH20	wt		no
RH21	wt		no
RH22	wt		no
RH23	wt		no
RH24	wt		no
RH25	possible change	wt	yes
RH26	possible change	wt	yes

Exon 5

Sample No.	Sequencing Conclusion	Sequenced?
RH01	c.752 C>T & c.831 T>C	yes
RH02	WT	yes
RH03	WT	yes
RH04	WT	yes
RH05	WT	yes
RH06	c.752 C>T & c.831 T>C	yes
RH07	WT	yes
RH08	WT	yes
RH09	c.831 T>C	yes
RH10	WT	yes
RH11	**c.831 T>C**	yes
RH12	WT	yes
RH13	c.831 T>C	yes
RH14	c.752 C>T & c.831 T>C	yes
RH15	WT	yes
RH16	WT	yes
RH17	WT	yes
RH18	WT	yes
RH19	WT	yes
RH20	WT	yes
RH21	c.831 T>C	yes
RH22	c.831 T>C	yes
RH23	WT	yes

RH24	c.831 T>C	yes
RH25	inconclusive	yes
RH26	WT	yes

Appendix B – Heteroduplex Analysis and Direct Seqencing of 47 healthy Controls (TACI exon 3 and exon 4 only)

Exon 3

Sample No.	HA prediction	Sequencing Conclusion	Sequenced?
BB001	Homo c.445+25A>C		no
BB002	possible change	Homo c.445+25A>C	yes
BB003	Het c.445+25A>C		no
BB004	wt		no
BB005	Het c.445+25A>C		no
BB006	wt		no
BB007	Het c.445+25A>C		no
BB008	Homo c.445+25A>C		no
BB009	Het c.445+25A>C		no
BB010	No change		no
BB011	Het c.445+25A>C		no
BB012	Het c.445+25A>C		no
BB013	Het c.445+25A>C		no
BB014	wt		no
BB015	Het c.445+25A>C		no
BB016	Homo c.445+25A>C		no
BB017	inconclusive	Het c.215G>A (R72H); c.445+25A>C	yes
BB018	Het c.445+25A>C		no
BB019	possible change	Homo c.445+25A>C	yes
BB020	wt		no
BB021	possible change	Het c.291T>G (Pro97) & c.445+25A>C	yes
BB022	possible change	No change	yes
BB023	Het c.445+25A>C		no
BB024	Het c.445+25A>C		no
BB025	wt		no
BB026	wt		no
BB027	Het c.445+25A>C		no
BB028	Homo c.445+25A>C		no
BB029	No change		no
BB030	Het c.445+25A>C		no
BB031	inconclusive	Het c.445+25A>C	yes
BB032	wt		no
BB033	wt		no
BB034	Het c.445+25A>C		no
BB035	Het c.445+25A>C		no
BB036	Het c.445+25A>C		no
BB037	Homo c.445+25A>C		no
BB038	possible change	Het c.291T>G & c.445+25A>C	yes
BB039	Homo c.445+25A>C		no
BB040	Het c.445+25A>C		no
BB041	Het c.445+25A>C		no
BB042	Het c.445+25A>C		no
BB043	Het c.445+25A>C		no
BB044	Het c.445+25A>C		no
BB045	Het c.445+25A>C		no
BB046	Homo c.445+25A>C		no

BB047	wt		no

Exon 4

Sample No.	HA prediction	Sequencing Conclusion	Sequenced?
BB001	wt		no
BB002	possible change	no change	yes
BB003	wt		no
BB004	possible change	no change	yes
BB005	possible change	no change	yes
BB006	wt		no
BB007	wt		no
BB008	wt		no
BB009	possible change	Het c.605G>A (R202H)	yes
BB010	wt		no
BB011	wt		no
BB012	wt		no
BB013	wt		no
BB014	wt		no
BB015	wt		no
BB016	possible change	no change	yes
BB017	wt		no
BB018	wt		no
BB019	wt		no
BB020	possible change	no change	yes
BB021	possible change	no change	yes
BB022	possible change	no change	yes
BB023	wt		no
BB024	wt		no
BB025	possible change	no change	yes
BB026	possible change	no change	yes
BB027	possible change	no change	yes
BB028	possible change	no change	yes
BB029	wt		no
BB030	wt		no
BB031	wt		no
BB032	wt		no
BB033	wt		no
BB034	wt		no
BB035	wt		no
BB036	possible change	Het c.563A>T (K188M)	yes
BB037	wt		no
BB038	wt		no
BB039	wt		no
BB040	wt		no
BB041	possible change	no change	yes
BB042	wt		no
BB043	wt		no
BB044	wt		no
BB045	wt		no
BB046	wt		no
BB047	wt		no